# Riemann Problems for the Two-Dimensional Unsteady Transonic Small Disturbance Equation

Sunčica Čanić*
Department of Mathematics
Iowa State University
Ames, Iowa 50011

Barbara Lee Keyfitz†
Department of Mathematics
University of Houston
Houston, Texas 77204-3476

Abstract. We study a two-parameter family of Riemann problems for the UTSD equation, also called the two-dimensional Burgers equation, which is used to model the transition from regular to Mach reflection for weak shock waves. The related initial-value problem consists of oblique shock data in the upper half plane, with two parameters $a$ and $b$ corresponding to the slopes of the initial shock waves. The study of quasi-steady solutions leads to a problem that changes type when written in self-similar coordinates. The problem is hyperbolic in the region where the flow is supersonic, and elliptic where the flow is subsonic.

In this paper we give a complete description of the flow in the hyperbolic region by resolving the hyperbolic wave interactions in the form of quasi-one-dimensional Riemann problems. In the region of physical space where the flow is subsonic, we pose the related free-boundary problems and discuss the behavior of the subsonic solution using results from our previous work. Based on this approach we establish the existence of regions of different qualitative behavior in parameter $(a, b)$ space. Our results reveal that the UTSD equation seems to be particularly suitable for the study of the so called von Neumann paradox in which linearly degenerate waves can be ignored. We establish the region in the parameter space where a prototype of von Neumann reflection takes place. In other regions of parameter space we find prototypes for Mach reflection, regular reflection, and transitional Mach reflection. The lack of linearly degenerate waves in this model is resolved by the presence of a small rarefaction wave emerging from the triple point.

Key words. Two-dimensional Riemann problems, unsteady transonic

*Supported by the Department of Energy, grant DE-FG02-94ER25220, and in part by the NSF under grant DMS-9403598. Support by the Energy Laboratory and the Department of Mathematics at the University of Houston is also acknowledged.

†Research supported by the Texas Advanced Research Program under Grant 00365-2102-ARP and the Department of Energy, grant DE-FG03-94ER25222.

small-disturbance equation.

AMS subject classification. Primary: 35L65, 35L37; Secondary: 35M10

Contents

**1. Introduction** **3**

**2. The Geometry of Primary Intersections** **5**

**3. Quasi-One-Dimensional Riemann Problems** **10**
3.1 The Shock Polar . . . . . 13
3.2 The Rarefaction Polar . . . . . 17
3.3 Solvable Quasi-One-Dimensional Riemann Problems . . . . . 19
3.4 The Hyperbolic Solution for Case 1 Parameters . . . . . 23

**4. Shock Reflection Problems for Other Parameter Values** **26**
4.1 Symmetric Shock Reflection at the Wall . . . . . 26
4.2 The UTSD Prototype for von Neumann Reflection . . . . . 31
4.3 Transitional Mach Reflection . . . . . 33
4.4 A Mechanism for Mach Reflection with a Kink . . . . . 35

**5. Conclusions** **37**

List of Figures

1 Riemann Data for a Shock Reflection Problem . . . . . 4
2 The Hyperbolic and Elliptic Regions in $(\xi, \eta)$ . . . . . 6
3 Sketch of Primary Intersection Points . . . . . 8
4 Classification of Parameter Space by Position of $\Xi_I$ . . . . . 10
5 Shock Polar Configurations for $U_0 = (1, -3)$ and $\Xi_0 = (2.5, 2.5)$ (top) and for $U_0 = (1, -3)$ and $\Xi_0 = (0.5, 0.5)$ (bottom) . . . 14
6 Characteristic and Shock Angles on Shock Polar for $U_0 = (1, -3), \Xi_0 = (2.5, 2.5)$ . . . . . 16
7 Admissible Configurations Along the Shock Polar . . . . . 17
8 The Rarefaction Polar at $U_0 = (1, -3); \Xi_0 = (2.5, 2.5)$ . . . . 19
9 Characteristic Angles on the Rarefaction Polar for $U_0 = (1, -3), \Xi_0 = (2.5, 2.5)$ . . . . . 20
10 A Centered Rarefaction Wave . . . . . 20
11 Downstream Locus and Solution Regions of Quasi-One-Dimensional Problems . . . . . 21

12 Riemann Solution for $U_2$ in Region Four and Boundary of the Subsonic Region . . . . . 23
13 Subregions of the Regular Reflection Region, $\mathcal{R}$ . . . . . 28
14 Uniform Regular Reflection, Upper Branch of $J$ . . . . . 29
15 Uniform Regular Reflection, Lower Branch of $J$ . . . . . 30
16 The Form of the Perturbed Reflection Problem in One Region (Subregion 4) . . . . . 30
17 Hyperbolic Solution in von Neumann Reflection . . . . . 32
18 Geometry of Primary Curves in Transitional Mach Reflection 33
19 Transitional Mach Reflection . . . . . 36
20 Wave Interaction Bifurcation Diagram . . . . . 38

## 1. Introduction

This paper reports on a study of the unsteady transonic small disturbance equation

$$\begin{aligned} u_t + uu_x + v_y &= 0\,, \\ -v_x + u_y &= 0\,. \end{aligned} \tag{1.1}$$

An initial summary was given in [9]. This equation models the transition between Mach and regular reflection for weak shocks and small wedge angles. Based on the work of Brio and Hunter, [3], we consider Riemann data consisting of three states in the upper half plane, separated by shocks. The boundary data on the $x$-axis are $u_y = 0 = v$. We consider the *oblique shock interaction problem* with states

$$\begin{cases} U_0 &= (0,0) \\ U_1 &= (1,-a) \\ U_2 &= (1+a/b,0) \end{cases} \tag{1.2}$$

(see Figure 1) and initial discontinuities on the lines $x = ay$ and $x = -by$. This results in discontinuities which propagate as shocks.

In this paper we show that the two-parameter problem displays qualitative features similar to those seen in a number of studies of shock interaction problems [2, 11, 12, 13, 14, 15, 16].

Most of this paper is devoted to solving and reducing the self-similar problem to the point where the subsonic problem can be identified and studied. In other work, we have begun an analysis of the subsonic problem, [4, 7, 6]. Based on our experience with this problem, we offer some conjectures on what the subsonic analysis may reveal. Numerical results in [10] confirm those conjectures. In Section 2 we propose a bifurcation diagram

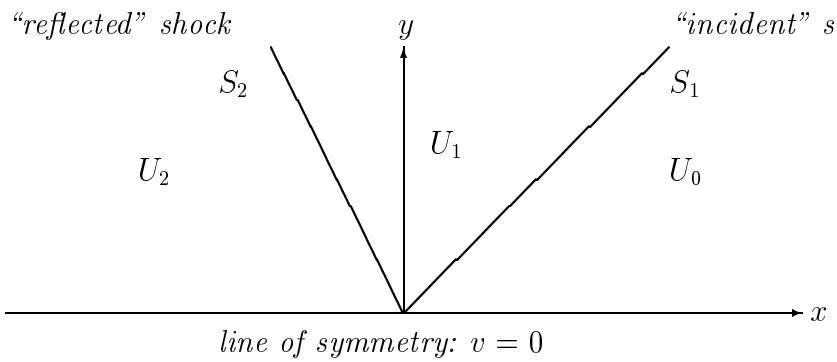


**Figure 1:** Riemann Data for a Shock Reflection Problem

in $(a, b)$-parameter space based on preliminary wave analysis. In Sections 3 and 4, we outline the free-boundary problems that arise in the interaction between hyperbolic waves and the subsonic (elliptic) region. We summarize our conclusions in Section 5 and give a revised bifurcation diagram based on hyperbolic wave interactions and subsonic flow behavior.

Our approach here, based strongly on similarity solutions and the corresponding dimension reduction that results, does not say anything about multi-dimensional flows which are not self-similar (quasi-steady). However, Riemann problems in one-dimensional gas dynamics have played a very important role which may extend to two-dimensional problems. In addition, self-similar solutions are used to model prototype shock reflection problems, as described above.

Self-similar analysis suggests that there may be more than one solution for certain configurations of data. We prove in Theorem 3.1 that this is indeed the case. This is in the nature of bifurcation problems. Because of the construction we are using, we believe that all the solutions we find and conjecture are stable to small perturbations of the Riemann data, to perturbation by smoothing of the data, or to viscous perturbation of the equations.

In self-similar coordinates, $\xi = x/t$, $\eta = y/t$, equation (1.1) becomes

$$\begin{aligned} (u-\xi)u_\xi - \eta u_\eta + v_\eta &= 0\,, \\ -v_\xi + u_\eta &= 0\,. \end{aligned} \tag{1.3}$$

This can be written as a quasilinear system

$$\begin{aligned} A(U,\Xi)U_\xi + B(U,\Xi)U_\eta &\equiv \left[\begin{pmatrix} u-\xi & 0 \\ 0 & -1 \end{pmatrix}\partial_\xi + \begin{pmatrix} -\eta & 1 \\ 1 & 0 \end{pmatrix}\partial_\eta\right]\begin{pmatrix} u \\ v \end{pmatrix} \\ &= 0 \end{aligned} \tag{1.4}$$

or in conservation form

$$\begin{aligned} \partial_\xi F(U,\Xi) + \partial_\eta G(U,\Xi) &\equiv \partial_\xi \begin{pmatrix} u^2/2 - \xi u \\ -v \end{pmatrix} + \partial_\eta \begin{pmatrix} v - \eta u \\ u \end{pmatrix} \\ &= S \equiv \begin{pmatrix} -2u \\ 0 \end{pmatrix} \end{aligned} \tag{1.5}$$

with $U = (u, v)$ and $\Xi = (\xi, \eta)$.

Now, from (1.4) it can easily be seen that the system changes type; it is hyperbolic outside and elliptic inside the parabola

$$P_u : \qquad \xi + \frac{\eta^2}{4} = u.$$

The characteristics in the hyperbolic region are straight lines (when the equation is linearized about a constant state) tangent to $P_u$. See Figure 2.

In addition, shocks between constant states, from (1.5) (see Section 3.1), have the form

$$\xi = \kappa\eta + \omega$$

where

$$\kappa \equiv -\frac{[v]}{[u]} = -\frac{v_L - v_R}{u_L - u_R}; \qquad \omega \equiv \kappa^2 + \frac{u_L + u_R}{2}.$$

In the next section we identify the geometry of the elementary configurations corresponding to the states in this problem.

## 2. The Geometry of Primary Intersections

The following geometric objects play a role in the analysis.

**Shocks:** $S_1$ (between $U_0$ and $U_1$): $\xi = a\eta + (1/2 + a^2) \equiv \kappa_1\eta + \omega_1$
$S_2$ (between $U_1$ and $U_2$): $\xi = -b\eta + (1 + a/2b + b^2) \equiv \kappa_2\eta + \omega_2$

**Parabolas:** $P_0$: $\xi = -\eta^2/4$
$P_1$: $\xi = -\eta^2/4 + 1$
$P_2$: $\xi = -\eta^2/4 + 1 + a/b$

(Each $P_i$ is the change of type locus for the state $U_i$.)

**Axis of Symmetry** $W$ (wall): $\eta = 0$

These six objects define the *primary curves* of the problem: they are intrinsically defined in terms of the quasi-one-dimensional data for the reduced problem (1.3). We consider the data for this problem to be "Cauchy

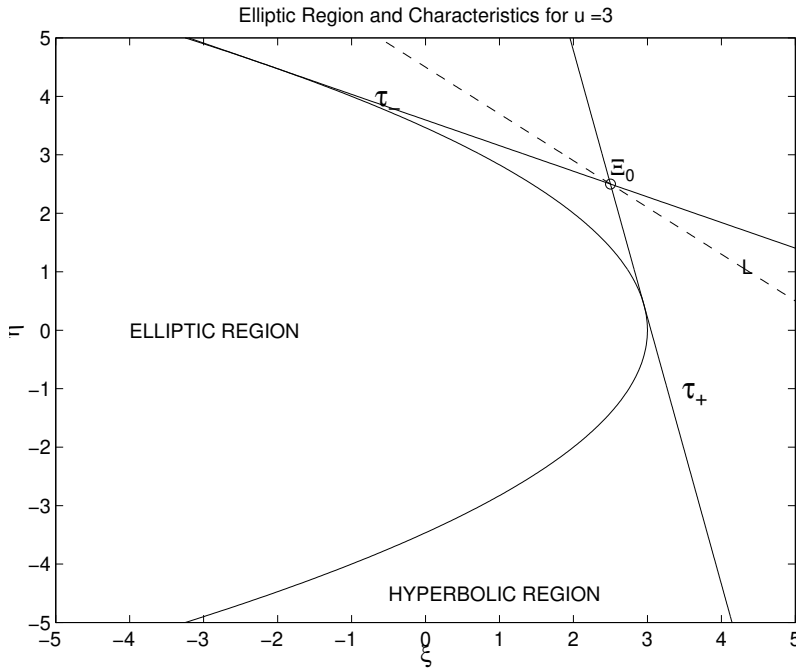


**Figure 2:** The Hyperbolic and Elliptic Regions in $(\xi, \eta)$

data given at infinity", corresponding to Riemann data for the original two-dimensional problem given at $t = 0$, since $|\Xi| \to \infty$ as $t$ decreases to zero. In fact, the negative $x$-axis is not appropriate for giving data, because (1.1) is not hyperbolic in time: we should consider data given on a parabolic arc

$$\xi + \eta^2/4 = C \tag{2.1}$$

for sufficiently large $C$. As long as we are considering simple data of the form (1.2) the exact nature of this curve is not important.

Using the linearized equation, we can define the *domain of influence* of a point to be the union of the forward wave cone through the point and the parabola. For a point $(\xi, \eta)$ one can also define the *domain of dependence* by following the characteristics of (1.4) back to (2.1). For arbitrary piecewise constant data at infinity (or on (2.1)) we can define the *quasi-one-dimensional domain of determinacy*: assuming all the quasi-one-dimensional Riemann problems can be solved locally (as in the next section), there is a region of $(\xi, \eta)$ space outside of (or "before") any intersections of the primary curves take place. To help in categorizing the different cases which may arise, we define

**Definition 2.1** *The* primary intersections *are all the points* $\Xi$ *at which the primary curves could intersect and generate new waves. These points, for*

| Intersection | Name | Point |
|---|---|---|
| $S_1 \cap S_2$ | $\Xi_I$ | $(1/2 + a/2b + ab, 1/2b + b - a)$ |
| $S_2 \cap P_2$ | $\Xi_0$ | $(1 + a/2b - b^2 - \sqrt{2ab}, 2b + \sqrt{2a/b})$ |
| | $\Xi_*$ | $(1 + a/2b - b^2 + \sqrt{2ab}, 2b - \sqrt{2a/b})$ |
| $S_1 \cap P_1$ | $\Xi_1$ | $(-a^2 + a\sqrt{2} + 1/2, -2a + \sqrt{2})$ |
| $S_1 \cap W$ | $\Xi_A$ | $(\omega_1, 0) = (1/2 + a^2, 0)$ |
| $S_2 \cap W$ | $\Xi_B$ | $(\omega_2, 0) = (1 + a/2b + b^2, 0)$ |
| $S_1 \cap P_2$ | | $(-a^2 + 1/2 + \sqrt{2a + 4a^2/b}, -2a + \sqrt{2 + 4a/b})$ |

**Table 1:** The Primary Intersections

*our problem, are* $S_1 \cap S_2$, $S_i \cap W$ *and* $S_i \cap P_i$ *for* $i = 1$ *and* 2.

For convenience, we label all points, even though some of them are in the lower half-plane for some parameter values. The list is in Table 1; a sketch in Figure 3 identifies the points.

**Remark**: It is clear that intersections of one shock with another, or of a shock with the wall, generate new waves. But the point where a shock intersects the parabola corresponding to one state of the shock may mark a transition from uniform to nonuniform flow, as we shall explore.

Not all the primary intersections actually occur in the solution of the Riemann problem; some never occur, and some occur or not depending on the values of $a$ and $b$. A primary intersection will occur if it is not in the domain of influence of any other intersection or of nonconstant data on (2.1). Because the characteristics in the hyperbolic region are easily computed (Figure 2), it is straightforward to compute the forward domain of influence of any point. The elliptic regions are conveniently nested, based on the magnitude of the data. However, there is no maximum principle: data at infinity may generate states of larger magnitude, and hence an *a priori* computation of the backwards domain of dependence of any point is not possible.

**Definition 2.2** *An* admissible intersection *is one that is completely determined by the data at infinity.*

We can determine the admissible intersections for different ranges of $a$ and $b$. The following elementary propositions were proved in [9].

**Proposition 2.1** *If* $\Xi_I$ *is upstream from* $\Xi_0$ *then it is admissible.*

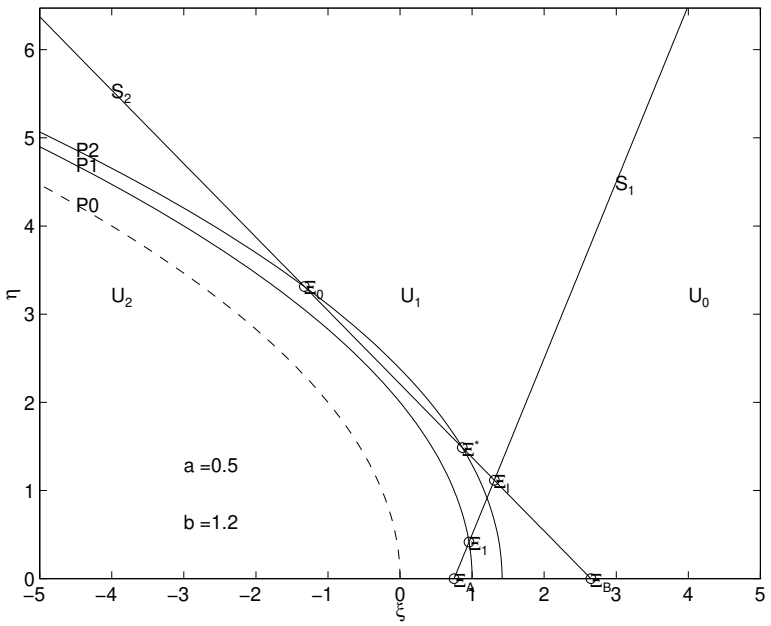


**Figure 3:** Sketch of Primary Intersection Points

Now, this occurs if $\eta_I \geq \eta_0$. This is the case if $b < 1/\sqrt{2}$ and

$$a \leq \frac{3}{2b} - b - \sqrt{2}\sqrt{\frac{1}{b^2} - 1} \equiv I(b).$$

Note that $\Xi_I$ is outside $P_2$ when

$$a^2 + (2b - 3/b)a + 1/(4b^2) + b^2 - 1 \equiv a^2 + (2b - \frac{3}{b})a + \left(\frac{1}{2b} - b\right)^2 > 0$$

which holds if $a$ is outside the roots of the quadratic, that is, if $a$ is not between

$$\frac{3}{2b} - b \pm \sqrt{2}\sqrt{\frac{1}{b^2} - 1}.$$

In particular, if $b > 1$, then $\Xi_I$ is always outside $P_2$. Let $K$ be the curve defined by

$$a = \frac{3}{2b} - b - \sqrt{2}\sqrt{\frac{1}{b^2} - 1}, \;\; 1/2 \leq b \leq 1$$

and

$$a = \frac{3}{2b} - b + \sqrt{2}\sqrt{\frac{1}{b^2} - 1}, \;\; 0 \leq b \leq 1.$$

Then $\Xi_I = \Xi_*$ along $K$. For points $(a, b)$ between $I$ and $K$, the intersection point $\Xi_I$ lies inside $P_2$; below $I$, it lies above $P_2$ and above $K$ it lies beyond or below $P_2$. The implication of "beyond" here is that when $S_2$ emerges from $P_2$ at $\Xi_*$ and continues, it is, effectively, going backward in time, since movement along it is movement in the direction of decrease of the timelike variable.

**Proposition 2.2** *The shocks meet at the wall if* $a = b + 1/2b \equiv J(b)$.

The curve $J$ does not intersect $I$, but intersects $K$ at the point

$$(a^*, b^*) \equiv \left( \sqrt{1 + \frac{\sqrt{5}}{2}}, \frac{\sqrt{1 + \sqrt{5}}}{2} \right) \tag{2.2}$$

The curve $K$ terminates at this point (since points outside the upper half plane do not have meaning in this problem). A classification of points $(a, b)$ with respect to $\Xi_I$ was given in [9], as follows.

**Case 1** The region below $I$: $\Xi_I$ above $P_2$.

**Case 2** The region above $I$, below $K$ and left of $J$: $\Xi_I$ inside $P_2$, above $W$.

**Case 3** The region above $K$ and left of $J$: $\Xi_I$ beyond $P_2$, above $W$.

**Case 4** The region right of $J$: $\Xi_I$ below $W$.

See Figure 4, where these curves are labelled.

Although $\Xi_I$ is an important point, it may not actually determine the qualitative behavior of the flow since $\Xi_I$ may fail to be admissible. We have the following results.

**Proposition 2.3** *In Case 1,* $\Xi_I$ *is the only admissible primary intersection.*

**Proposition 2.4** *In Cases 2, 3, or 4,* $\Xi_0$ *is an admissible primary intersection and* $\Xi_I$ *is not.*

**Proof:** The entire interior of $P_2$ is downstream from $\Xi_0$. In Case 2, all the other primary intersections are inside $P_2$. ■

In Cases 3 and 4 there may be one or two admissible primary intersections, depending on whether $\Xi_A$ is inside or outside $P_2$. Noting that $\Xi_A$ is outside $P_2$ if $\omega_1 \equiv 1/2 + a^2 > 1 + a/b$, we see that $\Xi_A$ is outside $P_2$ if

$$a > \frac{1}{2b} + \sqrt{\frac{1}{4b^2} + \frac{1}{2}} \equiv L(b).$$

The curve $L$ contains the point $(a^*, b^*)$ and divides Cases 3 and 4 into two subregions, "left" and "right".

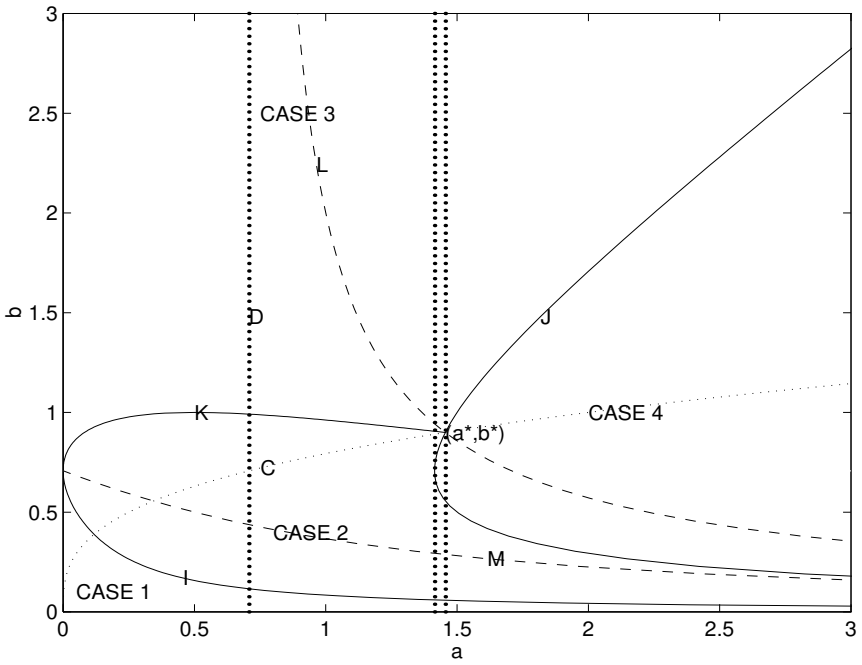


**Figure 4:** Classification of Parameter Space by Position of $\Xi_I$

**Proposition 2.5** *In either Case 3 or Case 4, if $(a, b)$ lies to the right of $a = L(b)$, there are two admissible primary intersections, $\Xi_0$ and $\Xi_A$. If $(a, b)$ lies to the left of this curve, there is only one admissible primary intersection, $\Xi_0$.*

In Case 1, one can construct a Mach reflection solution; in this paper we show how the primary intersections motivate the construction. In this case, the remaining step is to show that a certain degenerate elliptic free-boundary problem has a solution. We have solved the degenerate elliptic problem with a fixed boundary, finding a singular solution in [6] and a regular solution in [7], for different ranges of data. We can use these results to prove the existence of a solution to the free-boundary problem, [4].

To explain the construction of a solution in Case 1 and to obtain preliminary results in the other cases, we next study the quasi-one-dimensional Riemann problems which arise in this problem.

## 3. Quasi-One-Dimensional Riemann Problems

A quasi-one-dimensional Riemann problem has *data* consisting of a *center* $\Xi_0$ and two states, $U_1$, $U_2$ on a spacelike line, $L$, through a given point $\Xi_0$.

The *solution* is defined *downstream* from $L$. It is a function of

$$t \equiv \frac{\xi - \xi_0}{\eta - \eta_0}$$

defined in a forward half-space below $L$; it may be useful for the problem at hand only near $L$.

Now, an acceptable data line

$$L: \qquad (\xi - \xi_0)\cos\theta + (\eta - \eta_0)\sin\theta = 0$$

through $(\xi_0, \eta_0)$ with normal $\nu = (\cos\theta, \sin\theta) = (\lambda, \mu)$ must have the properties

1. Equation (1.4) is hyperbolic at $\Xi_0$ and
2. $\nu$ is a timelike (co)normal.

For property 1, $\det|A\lambda + B\mu| = 0$ must have two real roots. When $(U, \Xi_0)$ satisfy the condition

$$\xi_0 + \eta_0^2/4 - u > 0 \tag{3.1}$$

then

$$\frac{\mu}{\lambda} = \frac{\eta_0}{2} \pm \sqrt{\frac{\eta_0^2}{4} + \xi_0 - u} \tag{3.2}$$

are the two roots. Thus, to satisfy 1, a pair $(U, \Xi_0)$ must satisfy (3.1). In this case, the two lines through $\Xi_0$ with normals $(\lambda, \mu)_\pm$ given by (3.2) are the *characteristics*; they are the lines

$$\xi - \xi_0 + \left(\frac{\eta_0}{2} \pm \sqrt{\frac{\eta_0^2}{4} + \xi_0 - u}\right)(\eta - \eta_0) = 0,$$

which are lines through $\Xi_0$ tangent to the parabola $P_u$. (This fact was stated in Section 1 and can be seen by a straightforward calculation.)

**Definition 3.1** *We say that a pair* $(U, \Xi_0)$ *is a* hyperbolic pair *if condition* (3.1) *holds.*

The characteristics define the limiting slopes for spacelike lines; any straight line through $\Xi_0$ which does *not* intersect the parabola is spacelike. Furthermore, the side of the line which contains the parabola represents the "future" (forward time). Note that in (3.2) the choice of '+' gives a line

tangent to the upper half of the parabola (at a value $\eta > \eta_0$), and the choice '–' gives a point of tangency with $\eta < \eta_0$. A spacelike line is hence of the form

$$L: \qquad \xi - \xi_0 + \kappa(\eta - \eta_0) = 0 \text{ with } \left(\frac{\mu}{\lambda}\right)_+ > \kappa > \left(\frac{\mu}{\lambda}\right)_- . \tag{3.3}$$

This line may be vertical but is never horizontal; hence it always has a "left side", which corresponds to the future. A point $\Xi$ belongs to the future if $(\xi - \xi_0, \eta - \eta_0) \cdot (1, \kappa) < 0$; that is, $(1, \kappa)$ is a timelike normal in the *backwards* time direction. This explains property 2.

Now, for Riemann data, we may suppose we are given $(U_1, U_2, \Xi_0)$ with $\Xi_0$ outside $P_i$ (the parabola corresponding to $U_i$) for $i = 1, 2$, and a spacelike line $L$ as in (3.3). Since one parabola is inside the other, we need only verify the condition of being spacelike for the parabola with the larger value of $u$. For definiteness, we define the ordered data triple $(U_1, U_2, \Xi_0)$ to take the value $U_1$ on the lower half-line $\eta < \eta_0$ and $U_2$ on the upper.

The *solution* is a function

$$U(t) \equiv U\left(\frac{\xi - \xi_0}{\eta - \eta_0}\right)$$

defined in the *future*; that is, for

$$\xi - \xi_0 + \kappa(\eta - \eta_0) \equiv (t + \kappa)(\eta - \eta_0) \leq 0.$$

If we describe the solution to the Riemann problem by beginning at $t = -\kappa$ and $U = U_1$ on $L$, then $t$ increases to infinity (horizontal line) and then continues with $t$ increasing from $-\infty$ to $-\kappa$ again; at the final point, $U = U_2$ on $L$. This parameterization of the solution may appear somewhat awkward; however, the solution is always constant in a neighborhood of $t \to \pm\infty$.

Our aim is to describe the solution to the Riemann problem for all data. Now, at any $t$, $U(t)$ either

1. is constant in a neighborhood of $t$ or

2. has a shock at $t$ or

3. has a rarefaction in a (possibly one-sided) neighborhood of $t$.

Item 1 needs no explanation. We next describe shocks and rarefactions in turn.

### 3.1 THE SHOCK POLAR

If there is a shock on the line $\xi - \xi_0 = t(\eta - \eta_0)$, then from (1.5) we have the *Rankine-Hugoniot relation*:

$$F(U, \Xi_0) - F(U_0, \Xi_0) = t(G(U, \Xi_0) - G(U_0, \Xi_0))$$

where $U$ and $U_0$ are the constant states on either side of the discontinuity. Letting $[v] = v - v_0$ and so on, we have

$$\begin{aligned} \frac{1}{2}[u^2] - \xi_0[u] - t[v] + t\eta_0[u] &= 0 \\ -[v] - t[u] &= 0 \end{aligned}$$

so, immediately,

$$t = -\frac{v - v_0}{u - u_0} = -\frac{[v]}{[u]}; \qquad [v] = -[u]t. \tag{3.4}$$

Eliminating $t$ from the other equation, we get

$$\frac{[v]}{[u]} = \frac{\eta_0}{2} \pm \sqrt{\frac{\eta_0^2}{4} + \xi_0 - \left(\frac{u + u_0}{2}\right)}. \tag{3.5}$$

For (3.5) to have real solutions, we see that at least one of $(U, \Xi_0)$ and $(U_0, \Xi_0)$ must be a hyperbolic pair. Assuming that $(U_0, \Xi_0)$ is hyperbolic, then (3.5) defines the *shock polar*; it is defined for

$$u \le 2\left(\frac{\eta_0^2}{4} + \xi_0\right) - u_0 \equiv u_M; \tag{3.6}$$

and always forms a loop; there are two values of $v$ for each $u \neq u_0$, $u_M$, and those values are distributed above and below the line

$$\frac{[v]}{[u]} = \frac{\eta_0}{2},$$

which has positive slope if $\eta_0 > 0$. We denote the branches by $S^{\pm}$. The shock polar is also defined for pairs $(U_0, \Xi_0)$ which are not hyperbolic, but then it is not a loop; in this case $u_M < u_0$, and the locus consists of a single smooth branch and the isolated point $U_0$. See Figure 5.

To describe the shock polar, we introduce the following conventions. Fix $\Xi_0$ and $U_0$ so that $(U_0, \Xi_0)$ is a hyperbolic pair. Define the rightmost state on the shock polar:

$$U_M = (u_M, v_M) \equiv \left(2\left(\frac{\eta_0^2}{4} + \xi_0\right) - u_0, v_0 + \eta_0\left(\frac{\eta_0^2}{4} + \xi_0 - u_0\right)\right).$$

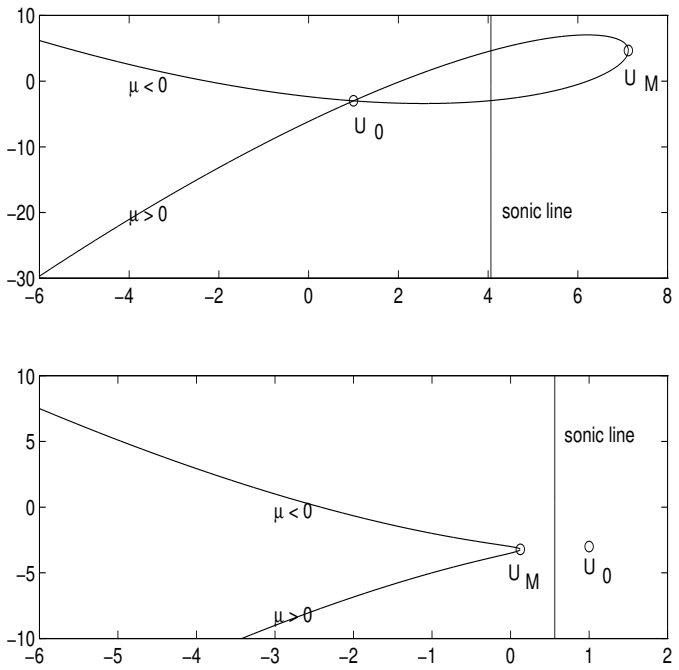


**Figure 5:** Shock Polar Configurations for $U_0 = (1, -3)$ and $\Xi_0 = (2.5, 2.5)$ (top) and for $U_0 = (1, -3)$ and $\Xi_0 = (0.5, 0.5)$ (bottom)

Define the parameter $\mu$ to be distance along the shock polar path from $U_M$, taken negative or positive according to the following convention:

$$\begin{cases} \mu < 0 \ \ (S^+): & \frac{[v]}{[u]} &= \frac{\eta_0}{2} - \sqrt{\frac{\eta_0^2}{4} + \xi_0 - \frac{u+u_0}{2}} \\ \mu > 0 \ \ (S^-): & \frac{[v]}{[u]} &= \frac{\eta_0}{2} + \sqrt{\frac{\eta_0^2}{4} + \xi_0 - \frac{u+u_0}{2}}. \end{cases} \tag{3.7}$$

Thus, $\mathrm{sgn}(du/d\mu) = -\mathrm{sgn}\mu$. As $\mu \to -\infty$, $[v]/[u] \to -\infty$ and as $\mu \to \infty$, $[v]/[u] \to \infty$. If $t$ denotes the shock angle[1] of the shock between $U$ and $U_0$, then

$$\begin{cases} \mu < 0 \ \ (S^+): & t &= -\frac{\eta_0}{2} + \sqrt{\frac{\eta_0^2}{4} + \xi_0 - \frac{u+u_0}{2}} \\ \mu > 0 \ \ (S^-): & t &= -\frac{\eta_0}{2} - \sqrt{\frac{\eta_0^2}{4} + \xi_0 - \frac{u+u_0}{2}}. \end{cases} \tag{3.8}$$

Note that

$$\frac{dt}{du} = \begin{cases} -\frac{1}{4}\left(\frac{\eta_0^2}{4} + \xi_0 - \frac{u+u_0}{2}\right)^{-1/2}, & \mu < 0 \\ \frac{1}{4}\left(\frac{\eta_0^2}{4} + \xi_0 - \frac{u+u_0}{2}\right)^{-1/2}, & \mu > 0 \end{cases}$$

[1] We refer to $t$ as a 'shock angle' throughout. It is actually the cotangent of the angle of the shock line to the horizontal.

and so $dt/d\mu < 0$ for all $\mu$. We use the following notation for the local characteristic angles:

$$\frac{\xi - \xi_0}{\eta - \eta_0} = -\left(\frac{\mu}{\lambda}\right)(U) \equiv \tau(U)$$

with

$$\tau_+(U) \equiv -\frac{\eta_0}{2} + \sqrt{\frac{\eta_0^2}{4} + \xi_0 - u} > -\frac{\eta_0}{2} - \sqrt{\frac{\eta_0^2}{4} + \xi_0 - u} \equiv \tau_-(U).$$

Note that the $\tau_-$ characteristic is tangent to the parabola *above* $\eta = \eta_0$, and the $\tau_+$ characteristic is tangent below (as illustrated in Figure 2). It is useful to define the *sonic points*. Let $u_s$ be the *sonic value*, where $\tau_\pm(U)$ becomes complex:

$$u_s = \frac{\eta_0^2}{4} + \xi_0$$

and note that $u_0 < u_s < u_M$; in fact,

$$u_M - u_s = \frac{\eta_0^2}{4} + \xi_0 - u_0 = u_s - u_0.$$

There are two sonic points, $U_{s\pm}$, on the shock polar, corresponding to $\mu$ positive or negative. Let $\mu_1 < \mu_2 < \mu_3 = 0 < \mu_4 < \mu_5$ be the values of $\mu$ corresponding to $U_0$ ($\mu_1$ and $\mu_5$), $U_s$ ($\mu_2$ and $\mu_4$) and $U_M$ ($\mu_3$). If we sketch all the quantities on a single graph, Figure 6, it is easy to see what types of shocks appear, and where.

The standard Lax geometric admissibility condition implies that $t$ in (3.8) must be between $\tau_+(U)$ and $\tau_+(U_0)$ for a +-shock (below the parabola) and between $\tau_-(U)$ and $\tau_-(U_0)$ for a −-shock (above); in addition *transonic* shocks are admissible if $U_0$ (the state with real characteristics) is upstream. Discussion of these admissibility conditions can be found in [5]. The state with the smaller value of $u$ is always upstream (on the right side of the shock, away from the smaller parabola). It is straightforward to check that in physical $(\xi, \eta)$ space, the shock line $t = (\xi - \xi_0)/(\eta - \eta_0)$ always intersects the outer parabola twice and is bounded away from the inner one.

For each value of $\mu$ there is a single admissible shock configuration, consisting of the triple $(U, U_0, t)$ (note this is all with respect to a fixed $\Xi_0$), and there are five intervals of qualitatively different behavior. They are

1. $\mu \in (-\infty, \mu_1)$: $\tau_+(U) > t > \tau_+(U_0)$; shock is *below* parabola $P_u$ and $U$ is *upstream*.

2. $\mu \in (\mu_1, \mu_2)$: $\tau_+(U_0) > t > \tau_+(U)$; shock is *below* parabola $P_0$ and $U_0$ is *upstream*.

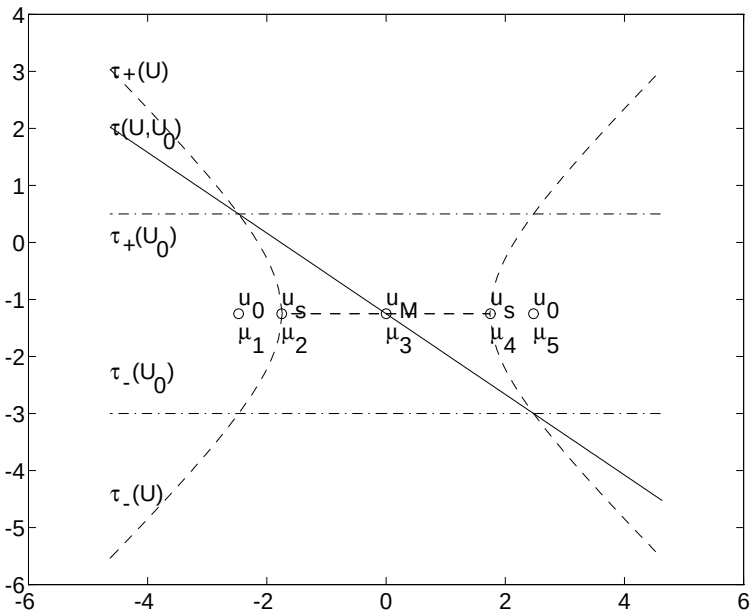


**Figure 6:** Characteristic and Shock Angles on Shock Polar for $U_0 = (1, -3), \Xi_0 = (2.5, 2.5)$

3. $\mu \in (\mu_2, \mu_4)$: $\tau_+(U_0) > t > \tau_-(U_0)$; $\tau_\pm(U)$ complex; $U_0$ is *upstream* and shock is transonic: neither above nor below; $\Xi_0$ is inside $P_u$.

4. $\mu \in (\mu_4, \mu_5)$: $\tau_-(U) > t > \tau_-(U_0)$; shock is *above* parabola $P_0$ and $U_0$ is *upstream*.

5. $\mu \in (\mu_5, \infty)$: $\tau_-(U_0) > t > \tau_-(U)$; shock is *above* parabola $P_u$ and $U$ is *upstream*.

An example from each of intervals 1 through 4 is sketched in Figure 7.

To use this information to solve quasi-one-dimensional Riemann problems with data $U_1$ and $U_2$ on $L$, note that the given states $U_1$ and $U_2$ must both be *upstream* states with respect to a shock joining them to adjacent states. Also, typically, the shock between $U_1$ and an adjacent state will be a $+$-shock (below the parabola: in interval 2 or 3) and that between $U_2$ and an adjacent state a $-$-shock (above: in interval 3 or 4). The 2-interval from $U_1$ will not intersect the 4-interval from $U_2$, unless $U_1$ and $U_2$ are correctly positioned relative to each other in the $u, v$ plane: $U_1$ must be more or less above $U_2$ and not too far away. Generally, the shock polars from $U_1$ and $U_2$ will intersect twice, so the intermediate state is not uniquely defined from the data. It is also clear that one case of interest, with Riemann data the

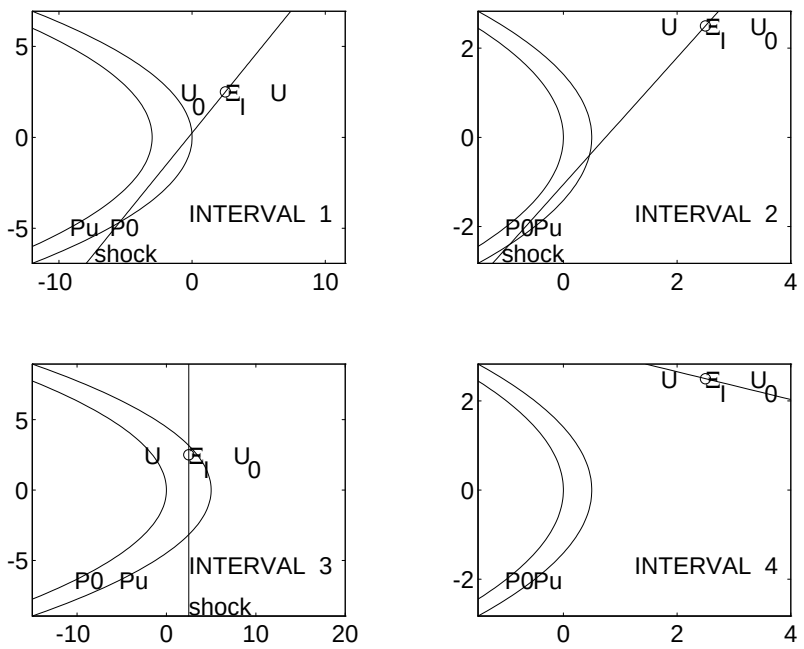


**Figure 7:** Admissible Configurations Along the Shock Polar

states $U_0$ and $U_2$ given by the original data, is not of this type, and the solution of this Riemann problem must also include rarefaction waves, which we now discuss.

### 3.2 The Rarefaction Polar

Centered simple waves are the third type of local solution $U(t)$ introduced at the beginning of Section 3. From (1.4) we obtain

$$(A - tB)U' = 0; \tag{3.9}$$

where now $' = d/dt$. Hence,

$$t = -\left(\frac{\mu}{\lambda}\right)_{\pm} \equiv \tau_{\mp}(U) = -\frac{\eta}{2} \mp \sqrt{\frac{\eta^2}{4} + \xi - u} = -\frac{\eta_0}{2} \mp \sqrt{\frac{\eta_0^2}{4} + \xi_0 - u},$$

where replacement of $\Xi$ in the formula by $\Xi_0$ is justified since the characteristic through $\Xi$ also goes through $\Xi_0$. Now $U'$ is a null vector of (3.9), so one finds (using the definitions of $A$ and $B$ in (1.4)) $tu' + v' = 0$ or

$$\frac{dv}{du} = -t = \frac{\eta_0}{2} \pm \sqrt{\frac{\eta_0^2}{4} + \xi_0 - u} = -\tau_{\mp}$$

(for the rarefaction curve corresponding to $\tau_\mp$), which we can integrate:

$$v(u) = \frac{\eta_0}{2}u \mp \frac{2}{3}\left(\frac{\eta_0^2}{4} + \xi_0 - u\right)^{3/2} + c$$

for the rarefaction curves through $\Xi_0$. Note that

$$\frac{dt}{du} = \pm\frac{1}{2}\frac{1}{\sqrt{\frac{\eta_0^2}{4} + \xi_0 - u}}$$

(the + sign refers to the $\tau_-$ root) and is positive for the $\tau_-$ root, and negative for the $\tau_+$ root.

We define $R(U_0, \Xi_0)$, the *rarefaction polar* connecting to $U_0$, centered at $\Xi_0$, by the formula

$$v = v_0 + \frac{\eta_0}{2}(u - u_0) \mp \frac{2}{3}\left\{\left(\frac{\eta_0^2}{4} + \xi_0 - u\right)^{3/2} - \left(\frac{\eta_0^2}{4} + \xi_0 - u_0\right)^{3/2}\right\}. \tag{3.10}$$

(The $-$ sign defines $R^-$, corresponding to $\tau_-$, the + sign gives $R^+$, corresponding to $\tau_+$.) Both $U$ and $U_0$ must be hyperbolic at $\Xi_0$, and the curves are defined for $u \le u_s = \eta_0^2/4 + \xi_0$. Unlike the shock polar, the rarefaction polar does not form a loop, but has two finite and two semi-infinite branches. For a sketch of the rarefaction curves, see Figure 8.

A picture of the local characteristic angles along $R(U_0, \Xi_0)$ (see Figure 9) can be used to construct a rarefaction wave configuration, as in Figure 10. There are four cases:

1. For an $R^-$ wave, $\tau_-(u) < \tau_-(u_0)$ if $U_0$ is the upstream state. Hence, the semi-infinite branch of $R^-$, with $u < u_0$, consists of states to which $U_0$ can be joined by a rarefaction, with $U_0$ the upstream state.

2. The other part of $R^-$, with $u_0 < u < u_s$, consists of $\tau_-$ waves where $U_0$ is now the downstream state.

3. On the $\tau_+$ branch, the rarefactions are tangent to the lower branches of the parabolas (as in Figure 10); again, the semi-infinite branch, $u < u_0$, contains states which are downstream from $U_0$.

4. On the part of $R^+$ with $u_0 < u < u_s$, $U$ is the upstream state (the case pictured in Figure 10).

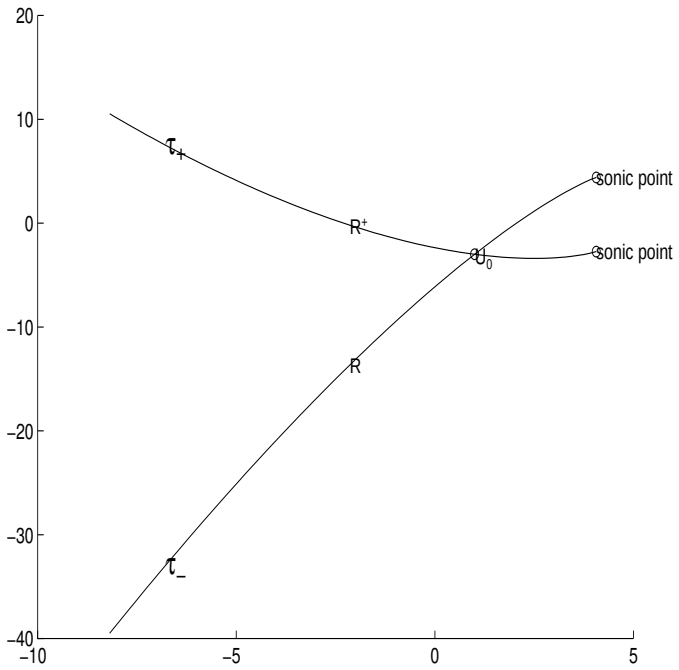


**Figure 8:** The Rarefaction Polar at $U_0 = (1, -3); \Xi_0 = (2.5, 2.5)$

### 3.3 SOLVABLE QUASI-ONE-DIMENSIONAL RIEMANN PROBLEMS

Unlike the standard one-dimensional Riemann problem, quasi-one-dimensional Riemann problems do not have solutions for all choices of $U_1$, $U_2$, and $\Xi_0$. Nor will the solution always be uniquely defined. However, we can give a precise result as follows.

Define the *downstream wave locus*, $D(U_1)$, of a state $U_1$, with respect to a fixed $\Xi_0$, as the union of all states which can be joined to $U_1$ by a shock or rarefaction in which $U_1$ is the upstream state. This locus is defined only if $U_1$ is a hyperbolic state. It consists of the loop part of the shock polar (intervals 2, 3, and 4), and the semi-infinite line segments from the rarefaction polar (intervals 1 and 3). Qualitatively, it looks like the shock polar; in particular, it extends beyond the line $u = u_s$. See Figure 11.

The downstream wave locus divides the half-plane $u \leq u_s$ into four regions, labelled 1 – 4 in Figure 11; we label the region above $U_1$ as '1' and continue counterclockwise. We can prove

**Theorem 3.1** *Given a Riemann data triple $(U_1, U_2, \Xi_0)$ with hyperbolic states $U_1$ on the lower half and $U_2$ on the upper half of a spacelike line $L$ through $\Xi_0$; let $D(U_1)$ be the downstream wave locus of $U_1$. Then if $U_2$*

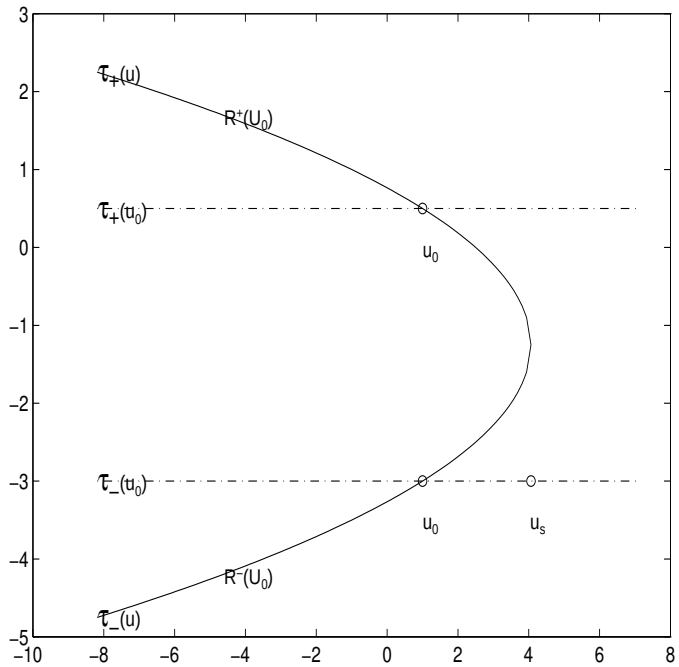


**Figure 9:** Characteristic Angles on the Rarefaction Polar for $U_0 = (1, -3), \Xi_0 = (2.5, 2.5)$

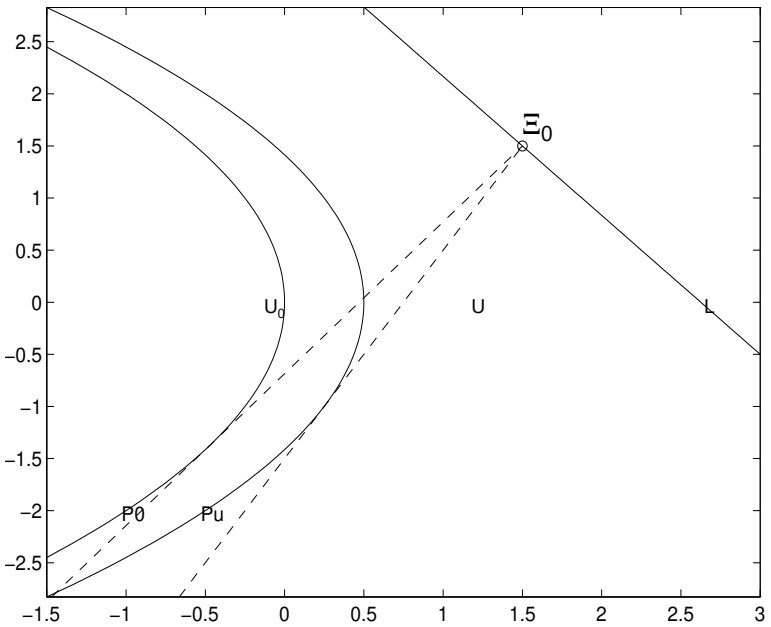


**Figure 10:** A Centered Rarefaction Wave

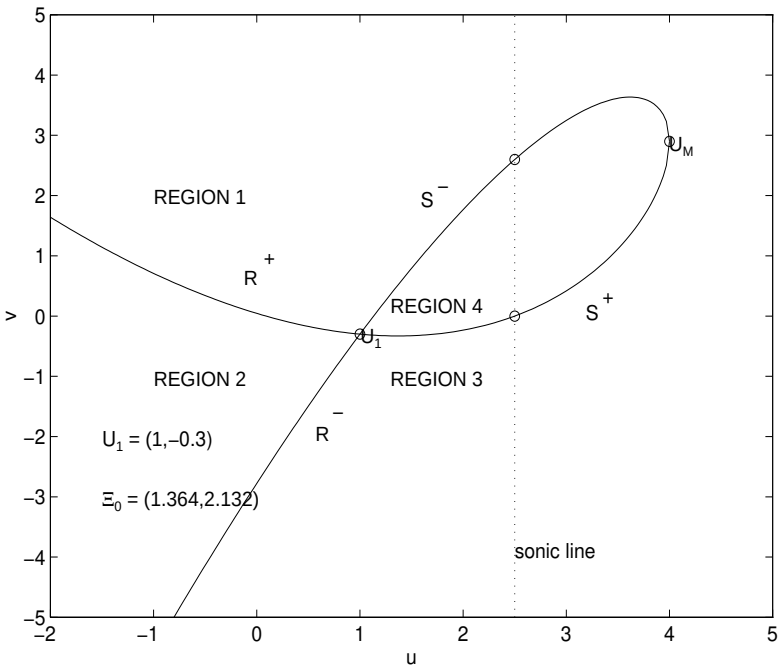


**Figure 11:** Downstream Locus and Solution Regions of Quasi-One-Dimensional Problems

*lies in any of the regions 1, 2, or 4 in the complement of $D(U_1)$, the Riemann problem has a unique admissible solution. If $U_2$ lies in region 3, there may be none, one or two admissible solutions.*

**Proof:** An admissible solution is a state $U_m$ on the intersection of $D(U_1)$ and $D(U_2)$ with the property that the wave angles are compatible with construction of a wave between $U_1$ and $U_m$ and another between $U_2$ and $U_m$. It is useful, in visualizing what points on the shock and rarefaction polars are associated with particular angles, to note that the equation $[v] = -[u]t$, (3.4), means that the shock angle, $t$, is orthogonal to the line segment joining $U_1$ to $U$ on $D(U_1)$ (for rarefactions, the corresponding equation is $dv/du = -t$, relating the wave angle to the tangent to the rarefaction polar). The fact that there are no horizontal waves corresponds to the nonexistence of vertical tangents or secants to the polars.

The three feasibility conditions on the angles $t_i$ of the waves between $U_i$ and $U_m$ ($i = 1, 2$) are

$$t_1 > \tau_-(U_1), \;\; t_2 < \tau_+(U_2), \;\; \frac{1}{t_1} > \frac{1}{t_2}.$$

The first implies that $U_m$ is not on $R^-(U_1)$, the second that $U_m$ cannot be

on $R^+(U_2)$. The third says that, with respect to $U_m$, four configurations of $U_1$ and $U_2$ are possible:

I. $U_1$ is left of $U_m$ and $U_2$ is also left of $U_m$ and below the line segment joining $U_m$ and $U_1$.

II. $U_1$ is left of $U_m$ and $U_2$ is right of $U_m$ and above the extension of the line segment joining $U_m$ and $U_1$.

III. $U_1$ is right of $U_m$ and $U_2$ is also right of $U_m$ and above the line segment joining $U_m$ and $U_1$.

IV. $U_1$ is right of $U_m$ and $U_2$ is left of $U_m$ and below the extension of the line segment joining $U_m$ and $U_1$.

All other arrangements are inadmissible.

Now, suppose $U_2$ is in region 1. We invoke standard theorems of ordinary differential equations to tell us that the $R^+$ and $R^-$ curves form smooth vector fields which cover the left half-plane without self-intersections; curves from opposite families intersect uniquely and transversely. A calculation, or use of a general result on convex shock curves, also tells us that intersections of shock loops with each other and with rarefaction curves are governed by exactly the mechanism one would see if the downstream locus were simply translated. Hence, when $U_2$ is in region 1 of Figure 11, there may be some intersections of shock curves, all of which are inadmissible, and there is always an intersection of $R^+(U_1)$ with $R^-(U_2)$; this produces a unique admissible point $U_m$ and a solution consisting of a pair of rarefaction waves.

If $U_2$ is in region 2, the unique admissible intermediate state $U_m$ is at the intersection of $R^+(U_1)$ and $S^-(U_2)$. This intersection always exists if $U_2$ is in region 2, for the shock loop of $U_1$ is inside the shock loop of $U_2$.

In region 4, which is bounded, the unique solution is the intersection of $R^-(U_2)$ and $S^+(U_1)$. This solution is illustrated in Figure 12.

However, in region 3, the only admissible points are the intersection of the shock loops $S(U_1)$ and $S(U_2)$. These points are the simultaneous solution, with $u_m > u_i$, of

$$\frac{v_m - v_1}{u_m - u_1} = \frac{\eta_0}{2} - \sqrt{\frac{\eta_0^2}{4} + \xi_0 - \left(\frac{u_m + u_1}{2}\right)}$$

(see equation (3.5)) and

$$\frac{v_m - v_2}{u_m - u_2} = \frac{\eta_0}{2} + \sqrt{\frac{\eta_0^2}{4} + \xi_0 - \left(\frac{u_m + u_2}{2}\right)}.$$

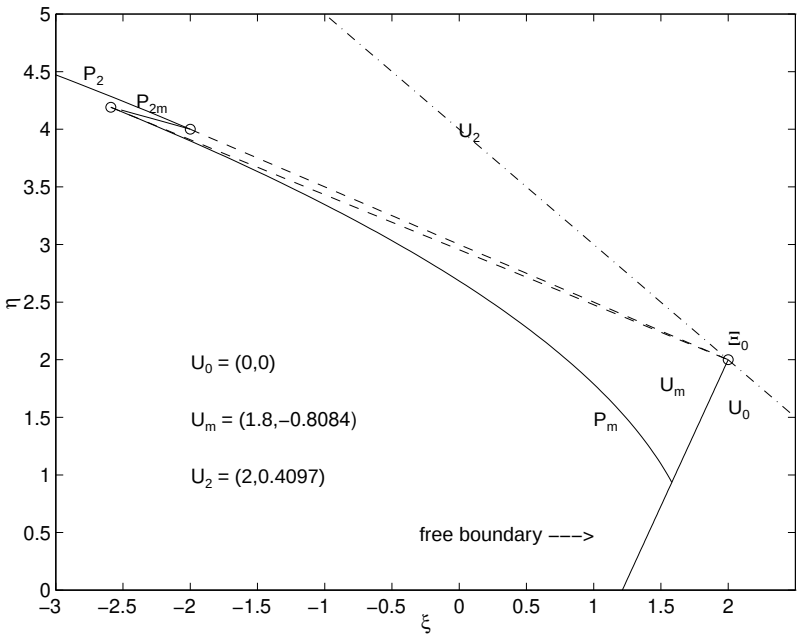


**Figure 12:** Riemann Solution for $U_2$ in Region Four and Boundary of the Subsonic Region

For fixed $u_1$ and $u_2$, if $v_1 - v_2$ is too large, there will not be a solution. Furthermore, except along a curve separating the region of no solutions, there will be two solutions. Again, typically, though not always, one solution will be supersonic and one subsonic. Standard admissibility criteria show that both are admissible. ■

### 3.4 The Hyperbolic Solution for Case 1 Parameters

Theorem 3.1 establishes the form of the solution of the hyperbolic Riemann problem which occurs when $(a, b)$ lies below the curve $I$ (Case 1 data).

**Theorem 3.2** *If oblique shock data* (1.2) *given for equation* (1.1) *are such that* $a \leq I(b)$*, then a hyperbolic quasi-one-dimensional Riemann problem occurs at* $\Xi_I$*. Furthermore, the data for this problem lead to a region 4 configuration, and there is a unique admissible solution, which consists of a rarefaction wave and a shock.*

**Proof:** The Riemann problem has data $U_0$ below $\Xi_I$ and $U_2$ above; here for $L$ we take any spacelike line. Because $\Xi_I$ is outside $P_2$ by hypothesis, the Riemann data is hyperbolic. Now, $U_2 = (1 + a/b, 0)$ lies directly to the

right of $U_0 = (0,0)$. We claim that this point is in region 4. Because of the remarks following equation (3.6), it is in either region 3 or 4, and it is in region 4 if the curve $S^+(U_0)$ lies below the $u$-axis at $u = u_2$. But on $S^+(U_0)$, from (3.5),

$$v = u\left(\frac{\eta_I}{2} - \sqrt{\frac{\eta_I^2}{4} + \xi_I - \frac{u}{2}}\right) \tag{3.11}$$

and $v(u_2) < 0$ if $\xi_I > u_2/2$. Checking the value of $\xi_I$ in Table 1 shows that this is indeed the case.

This construction can also be used to estimate the values of $v_m$ and $u_m$. We find $\xi_I - u_2/2 = a/2b$. This can be made arbitrarily small, and hence $v(u_2)$ in equation (3.11) arbitrarily close to zero, by choosing $a$ small relative to $b$. Then $R^-(U_2)$ will intersect $S^+(U_0)$ very close to $U_2$ (it can be checked that the slope of $R^-(U_2)$ is of order unity in this case); that is, $v_m$ is negative and near zero, while $u_m$ is less than $u_2$ and very close to $u_2$. ■

In fact, this solution gives a solution to the shock interaction problem at every point in the $(\xi, \eta)$ plane which is supersonic. We have

**Theorem 3.3** *The Riemann problem (1.2) for the unsteady transonic small disturbance equation (1.1) has a solution consisting of shocks, constant states and centered rarefaction waves in the exterior of the parabola $P_m$, defining the elliptic region for the state $U_m$, if the data $(a, b)$ are of Case 1 type.*

**Proof:** The solution outside $P_m$ is constructed by continuing the rarefaction wave joining $U_2$ to $U_m$ out to infinity, and then letting $U = U_m$ be constant below the rarefaction and between the rarefaction and the shock, outside $P_m$. When the shock enters $P_m$ it is expected to bend; inside $P_m$ one can formulate a problem for (1.1) which is elliptic inside the region and degenerate elliptic on the boundary. Data along the $\xi$ axis are chosen to be symmetric: $u_\eta = 0 = v$. The continuation of the shock, satisfying the Rankine-Hugoniot condition and with the constant state $U_0$ upstream, leads to a free-boundary problem. ■

The degenerate elliptic problem is solved in [7] and [6] and we are currently studying the free-boundary problem, [4].

The solution constructed this way is not unique, even in the hyperbolic region, since we continued the rarefaction fan beyond the parabolas. This violates causality: the infinite rays extend in the backwards timelike direction. An alternative and more physical construction terminates each ray in the rarefaction fan at the point where it becomes sonic. Then it

becomes necessary, to complete the problem, to find the nonuniform subsonic solution in the strip between $P_2$ and $P_m$. This changes the degenerate part of the boundary in the free-boundary problem mentioned above. The free-boundary problem for the position of the transonic shock between the upstream state $U_0$ and a subsonic state $U$ remains the same, but the region is now bounded by a part of the sonic parabola $P_2$, a part of the sonic parabola $P_m$, the wall, and a sonic curve $P_{2m}$ along which the states in the rarefaction wave between $U_2$ and $U_m$ become sonic. If $(\xi_I, \eta_I)$ denote the coordinates of $\Xi_I$, the equation for the curve $P_{2m}$ is given by

$$\xi - \xi_I = \frac{\eta}{2}(\eta_I - \eta). \tag{3.12}$$

Figure 12 pictures the corresponding hyperbolic solution and the boundary components for the elliptic problem. Equation (1.1) is elliptic inside the region where the flow is subsonic, and degenerate on the boundary $P_2 \cup P_m \cup P_{2m}$. We have not yet attempted to solve this problem for two reasons. First, we wish to understand the degenerate free-boundary problem, and so we have chosen a simplified problem to solve. In addition, $P_m$ is close to $P_2$, so this ambiguous region is small, and should not affect the existence of the solution in the interesting region near the free boundary. (However, to describe some more complicated wave interactions, as we outline in Section 4, we assume this more physical problem has a solution as well.)

A second reason for not considering the details of the problem near the tail of the parabola is that, as mentioned at the beginning of the paper, the original problem is not hyperbolic in time, and the ill-posedness centers about the treatment of the negative $\xi$-axis. If we were to consider, instead of (1.1), a problem such as the nonlinear wave equation, the nature of the difficulty in this region (now confined to a finite part of the plane) becomes clearer, and needs to be analysed.

We conclude this section with a remark about the wave interaction which occurs in the limit of Case 1, when $(a, b)$ lies on the curve $I$.

**Remark: (The Hyperbolic Solution for $(a, b) \in I$)** In this case $\Xi_I = \Xi_0 = \Xi_1$ and this is a limiting case in which $\Xi_I$ is still an admissible primary intersection. The shock $S_2$ is sonic at $\Xi_I$ and so we call the interaction between $S_1$ and $S_2$ at $\Xi_I$ a *degenerate hyperbolic wave interaction.* We solve this degenerate hyperbolic problem in the same way as for Case 1 data. By Theorem 3.2, the data for this problem leads to a region 4 configuration of wave curves and the solution consists of a $-$-rarefaction wave from $U_2$ to a state $U_m$ with $u_2 > u_m$, followed by a $+$-shock between $U_m$ and $U_0$.

In the more physical solution (where the characteristics in the rarefaction fan terminate at the sonic points), the rarefaction wave consists of characteristics whose lengths decrease to zero as $u \to u_2$.

To complete the solution we again need to solve a free-boundary problem for the position of the transonic shock between $U_0$ and the subsonic state $U$ in the domain whose boundary has the same constituents as in Case 1 data. The degenerate boundary consists of the parabola $P_2$, the curve $P_{2m}$, given by equation (3.12), along which the rarefaction wave is sonic, and the parabola $P_m$ across which $U_m$ changes from supersonic to subsonic. Even in this degenerate case, the component $P_{2m}$ of the degenerate boundary where $U$ is nonconstant is not adjacent to the free boundary.

## 4. Shock Reflection Problems for Other Parameter Values

In the preceding section, we showed how the problem of Mach stem formation reduces to a hyperbolic Riemann problem when the initial shocks at infinity fall into Case 1 (this is the case of almost vertical shocks). The quasi-steady problem in this particularly straightforward case is simplified by the fact that $\Xi_I$ is an admissible primary intersection; in fact, it is the only one, and it organizes the entire problem.

Outside this case, the behavior at $\Xi_I$ does not determine the problem; in fact, $\Xi_I$ may not even occur. There are four other modes of shock interaction which we can set up in some regions of space (possibly overlapping). We have not yet solved the corresponding elliptic problems for these cases, but we formulate them here, leaving the rest of the investigation to the future.

We begin by discussing another shock reflection problem, which may be hyperbolic, and may be primary, for some values of $a$ and $b$. We recall that Proposition 5 shows that $\Xi_A$ is a primary intersection if $(a, b)$ lies to the right of the curve $L(b)$ in Figure 4.

### 4.1 Symmetric Shock Reflection at the Wall

The interaction of the incident shock, $S_1$, with the wall may be reduced to a standard Riemann problem by considering as Riemann data at $\Xi_A = (\omega_1, 0)$ a spacelike line $L$ (a vertical line through $\Xi_A$) and data $U_1$ on the upper half of the line and the reflected state $U_1^* \equiv (1, a)$ on the lower half.

**Proposition 4.1** *This is a hyperbolic problem if* $a \geq 1/\sqrt{2}$.

**Proof:** The states $U_1$ and $U_1^*$ are hyperbolic at $\Xi_A$ if $u_1 = 1 \leq \xi_A = \omega_1$, or $a^2 \geq 1/2$. ■

However, for data of this form, if we consider the downstream locus, $D(U_1^*)$, for the value on the lower half-line, then $U_1$ is in region 3 of Theorem 3.1, where we are not guaranteed existence or uniqueness of a solution. For

the simple, symmetric data we consider here, the condition for existence is easy to derive. In fact, we have

**Proposition 4.2** *The quasi-one-dimensional Riemann problem with the data triple* $(U_1^*, U_1, \Xi_A)$ *has a solution if and only if* $a \geq \sqrt{2}$. *If* $a > \sqrt{2}$, *there are two solutions:*

$$U_R = (1 + a^2 - a\sqrt{a^2 - 2}, 0) \tag{4.1}$$

$$U_F = (1 + a^2 + a\sqrt{a^2 - 2}, 0). \tag{4.2}$$

**Proof:** The shock polar of $U_1$ has the equation (from (3.5))

$$\frac{v + a}{u - 1} = \pm\sqrt{\frac{1}{2} + a^2 - \frac{u + 1}{2}} \tag{4.3}$$

and by symmetry the solution to the Riemann problem must have an intermediate state with $v = 0$. Solving for $u$ we find (eliminating the solution $u = 0$)

$$u = 1 + a^2 \pm a\sqrt{a^2 - 2}$$

from which we get (4.1) and (4.2). ■

The intermediate state is hyperbolic if $u < \xi_A \equiv \frac{1}{2} + a^2$. Hence $U_F$ is never hyperbolic, while $U_R$ is hyperbolic if

$$a \geq \left(1 + \frac{\sqrt{5}}{2}\right)^{\frac{1}{2}} \equiv a^*$$

where $a^*$ is identified in equation (2.2). Since $a^* > \sqrt{2}$, there is a narrow range of $a$ in which both solutions (4.1) and (4.2) are elliptic (subsonic at $\Xi_A$); for larger $a$, only the state with larger magnitude is elliptic.

Let us identify the shock between $U_1$ and $U_R$ by the name $S_R$ ($R$ stands for 'reflected'; $F$ will stand for 'fast reflected' in (4.2)). The shock has the equation

$$\xi = \kappa_R \eta + \omega_R, \text{ where } \omega_R = \xi_A = \frac{1}{2} + a^2 \text{ and } \kappa_R = -\frac{1}{a - \sqrt{a^2 - 2}}.$$

Similarly, the shock between $U_1$ and $U_F$ is $S_F$, with

$$\xi = \kappa_F \eta + \omega_F, \text{ where } \omega_F = \xi_A = \frac{1}{2} + a^2 \text{ and } \kappa_F = -\frac{1}{a + \sqrt{a^2 - 2}}.$$

We now formulate the perturbed regular reflection equations. These equations can be formulated for all $a \geq \sqrt{2}$ and $a > I(b)$. We shall call this region of parameter space $\mathcal{R}$. We note that only if $a > L(b)$ is $\Xi_A$ an admissible primary intersection, but that it is always *locally admissible* in $\mathcal{R}$: that is, it lies outside of and upstream from $P_1$.

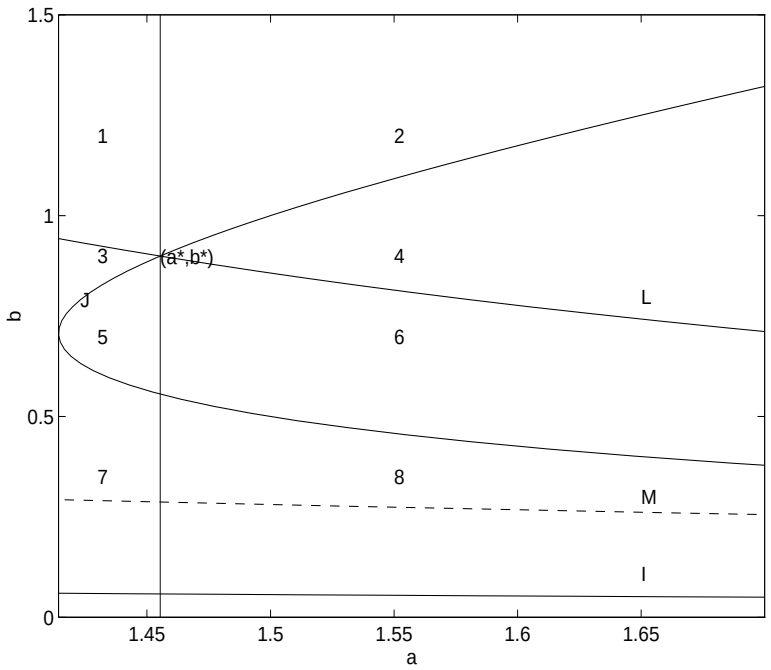


**Figure 13:** Subregions of the Regular Reflection Region, $\mathcal{R}$

**Proposition 4.3** *The curve $J(b)$ divides $\mathcal{R}$ into three regions:*
*top: $b > 1/(a - \sqrt{a^2-2})$, and $u_2 < u_R < u_F$*
*middle: $1/(a - \sqrt{a^2-2}) > b > 1/(a + \sqrt{a^2-2})$, and $u_R < u_2 < u_F$*
*bottom: $b < 1/(a + \sqrt{a^2-2})$, and $u_R < u_F < u_2$.*
*On the boundaries, we have*

$$b = \frac{1}{a - \sqrt{a^2-2}}, \exists \text{ uniform solution } U_2 = U_R, S_2 = S_R \tag{4.4}$$

$$b = \frac{1}{a + \sqrt{a^2-2}}, \exists \text{ uniform solution } U_2 = U_F, S_2 = S_F. \tag{4.5}$$

The line $a = a^*$ and the curve $a = L(b)$ also demarcate regions of potentially different behavior in $\mathcal{R}$. These three curves divide $\mathcal{R}$ into eight subregions, as shown in Figure 13.

For reference, we also draw a diagram of the uniform reflected shock solutions on the boundaries, using (4.4) and (4.5). The important point is to note where the boundaries of the super- and subsonic regions lie, since this is where perturbed solutions are expected to become nonuniform. See

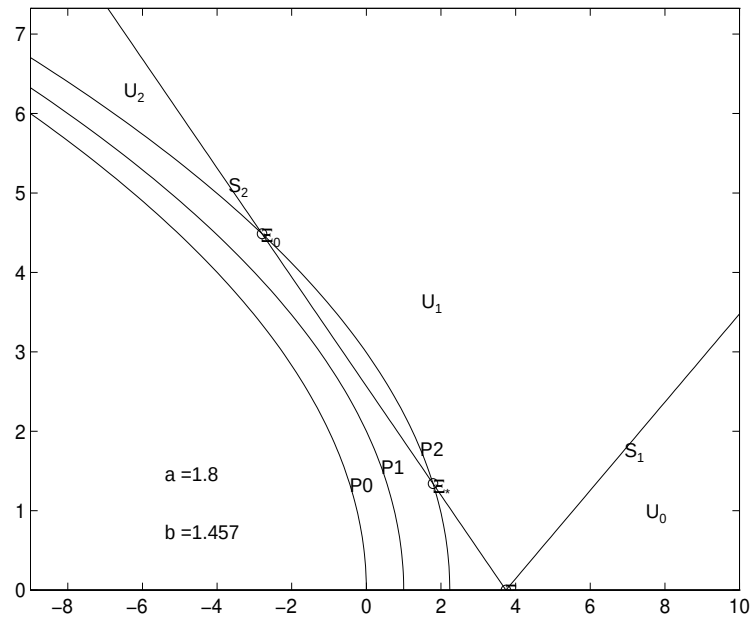


**Figure 14:** Uniform Regular Reflection, Upper Branch of $J$

Figures 14 and 15, which are drawn for a value of $a$ larger than $a^*$: the first sketch is on the boundary between subregions 2 and 4 in Figure 13, the second divides subregions 6 and 8.

It is plausible that for points $(a, b)$ near (4.4) or (4.5) there will be a solution close to the respective uniform solutions. In fact, however, we can define two perturbation problems at each point in $\mathcal{R}$, one based on each of the two Riemann solutions at $\Xi_A$. In both cases, the solution will be piecewise constant outside an elliptic region, in which the solution will satisfy a degenerate elliptic free-boundary problem. The exact nature of the problem varies depending on which Riemann solution is selected and which of the eight subregions we are in. We conjecture that only for some of these problems will solutions exist; thus, there may be two, one or even no regular reflection type solutions for $(a, b)$ in $\mathcal{R}$. Figure 16 describes the setup of the problem in one typical case (subregion 4).

In each case, the solution takes the following form: the shock $S_2$ is straight until it reaches the point $\Xi_0$, an admissible primary interaction. Then it continues as a curved shock. It eventually joins the point $\Xi_A$, which is therefore admissible in each case. What happens near $\Xi_A$ depends on whether we are perturbing a Riemann solution which is subsonic at $\Xi_A$ (the solution $U_F$ in all cases and the solution $U_R$ for values of $a$ between $\sqrt{2}$

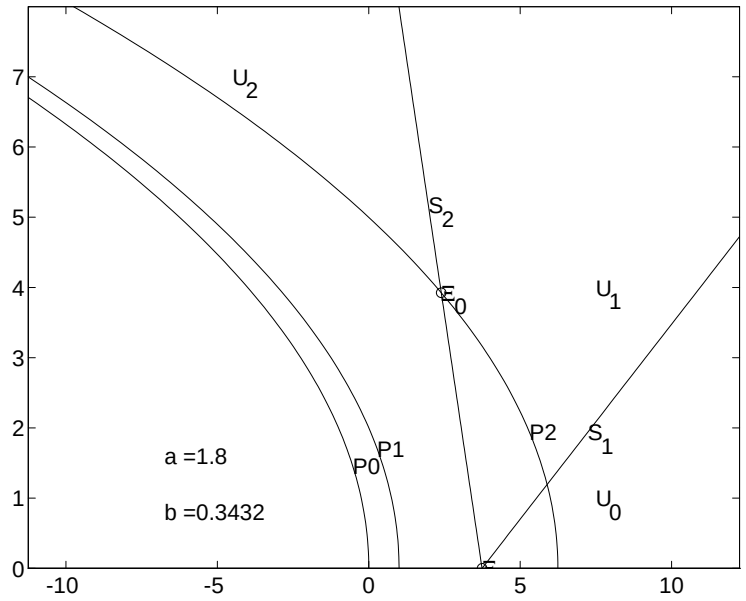


**Figure 15:** Uniform Regular Reflection, Lower Branch of $J$

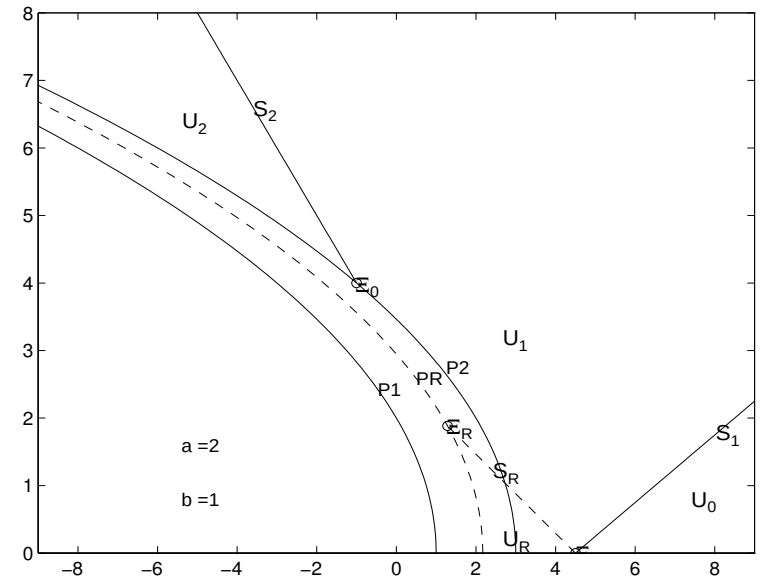


**Figure 16:** The Form of the Perturbed Reflection Problem in One Region (Subregion 4)

and $a^*$) or supersonic (the solution $U_R$ when $a > a^*$). Figure 16 shows the second possibility: the Riemann problem at $\Xi_A$ has a solution with middle state $U_R$ and reflected shock $S_R$. The pair $(U_R, \Xi_A)$ is hyperbolic, and thus the solution $U$ is constant in a wedge outside the parabola $P_R$ corresponding to $U_R$. A calculation shows that $S_R$ intersects $P_R$ at $\Xi_R$, where

$$\eta_R = \frac{2}{a - \sqrt{a^2 - 2}} \left(1 - \sqrt{a^2(2a^2 - 3) - a(2a^2 - 1)\sqrt{a^2 - 2}}\right)$$

and $\xi_R = \kappa_R \eta_R + \xi_A$. Between $\Xi_0$ and $\Xi_R$ the shock is curved: it satisfies a free-boundary problem (based on the Rankine-Hugoniot equation) with the constant state $U_1$ upstream and an elliptic solution to (1.1) downstream. The elliptic problem has two degenerate boundaries: $U = U_2$ along $P_2$ between $\Xi_0$ and $-\infty$, and $U = U_R$ along $P_R$ between $\Xi_R$ and $\eta = 0$. The $\xi$-axis is an axis of symmetry of the problem, along which one has the boundary conditions $u_\eta = 0 = v$, and a boundary condition must be applied at the infinite boundary. The only other comment about this problem is that the relative position of the two parts of the degenerate boundary may affect the type of solution (singular [6] or regular [7]) to be expected: the two possibilities are $u_2 > u_R$ (subregions 4, 6, and 8) or $u_2 < u_R$ (subregion 2).

Although this solution is based on perturbing the uniform regular reflection, the perturbation is by no means small unless $(a, b)$ is close to (4.4), and for $a > a^*$, and even then the solution may have a square root singularity at a point on the degenerate boundary as seen in [10].

If the Riemann solution at $\Xi_A$ is subsonic, then the shock from $\Xi_0$ remains transonic all the way to $\Xi_A$. The elliptic problem now resembles the problem considered in [4] except that the bottom point, solution value and shock angle on the free boundary are now fixed.

### 4.2 The UTSD Prototype for von Neumann Reflection

There is another region of parameter space where we can reduce the problem to solving an elliptic equation. This is the case where $\Xi_1 \equiv S_1 \cap P_1$ is admissible. This requires the two conditions $\eta_1 > 0$ (so that $\Xi_1$ exists) and $a > I(b)$, so that $\Xi_I$ is not admissible. The first condition, from Table 1, is $a < 1/\sqrt{2}$.

We describe the following reduction of the problem to a degenerate elliptic equation. Figure 17 pictures the important variables.

The solution has the constant value $U_2$ left of the shock $S_2$ up to the parabola $P_2$; the shock then becomes nonuniform, decaying and turning until it intersects $S_1$. At or before the point of intersection with $S_1$ it has

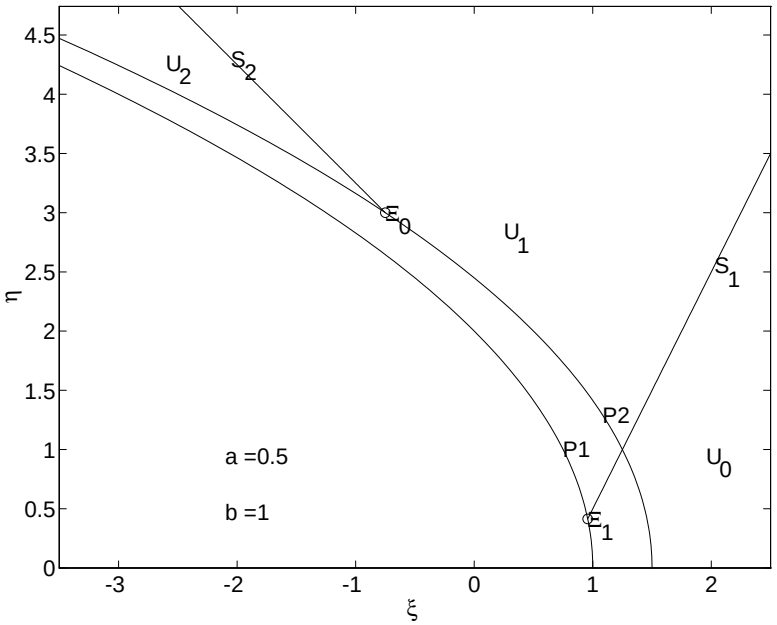


**Figure 17:** Hyperbolic Solution in von Neumann Reflection

zero strength. We expect this configuration to occur if $S_1$ intersects $\widetilde{S_2}$ after $\widetilde{S_2}$ becomes tangent to some sonic parabola $P_T$. Assuming small changes in the velocity $u$, and therefore even smaller changes in the position of the nonuniform shock, $\widetilde{S_2}$, (since the shock position is determined, via Rankine-Hugoniot conditions, as an integral of the velocity field), we replace $\widetilde{S_2}$ by $S_2$ to get an estimate for when this is the case. A simple calculation shows that the point of tangency, $\Xi_T$, is given by

$$\Xi_T = \left(1 + \frac{a}{2b} - b^2, 2b\right).$$

Therefore, we require that $(a, b)$ lie above the curve $M$ determined by the equation $\Xi_T = \Xi_I$:

$$a = M(b) \equiv \frac{1}{2b} - b. \tag{4.6}$$

This means, again supposing deviation from uniform flow is small, that the point $\widetilde{\Xi_I} = S_1 \cap \widetilde{S_2}$ lies on the right of $\Xi_T$.

Now, the shock $S_1$ is uniform until it reaches $P_1$; then it forms a free boundary between a nonuniform, subsonic solution and the upstream state $U_0$. As in the Mach stem case ([6], [8]), we expect the value of $u$ at the foot of the shock to be larger than $u_1 = 1$; thus $u = 1$ is the minimum value of $u$

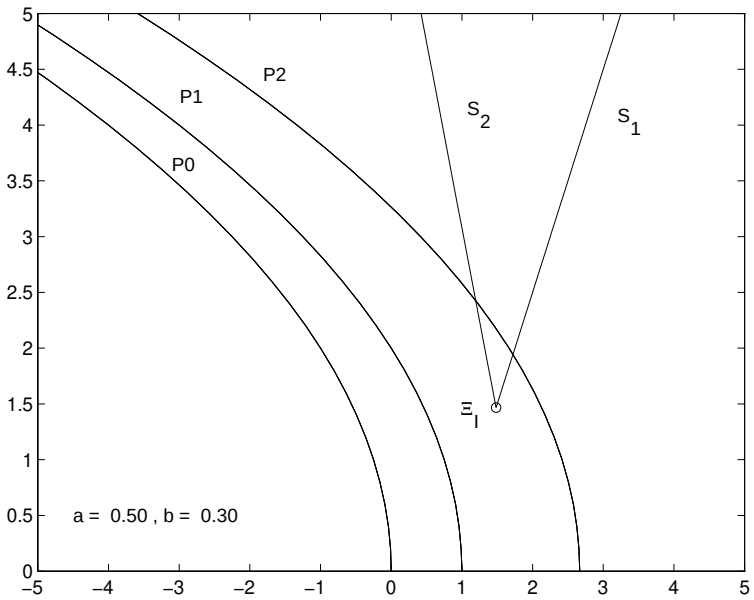


**Figure 18:** Geometry of Primary Curves in Transitional Mach Reflection

and is attained on the degenerate boundary, which we therefore expect to be singular. The elliptic problem in this case has two degenerate parts to its boundary – at $P_2$ and at $P_1$ – and two free-boundary problems arise. We expect that the solution at the degenerate boundary $P_1$ has a square-root type singularity at the point $\Xi_1$ where the shock $S_1$ intersects the sonic parabola $P_1$. Indeed, in [8] we showed that if the Mach stem $\xi = \xi(\eta)$ is an increasing, convex function, then the subsonic solution $u$ is a decreasing function of $\eta$ along the shock, and it must have a square-root singularity at the point where the Mach stem intersects the sonic curve. Numerical experiments in [10] confirm this scenario.

### 4.3 Transitional Mach Reflection

In the neighborhood of the region in $(a, b)$-parameter space in which Mach reflection takes place (Case 1), we expect to see a transition from Mach reflection to other types of reflection. In this spirit we pose the corresponding free-boundary problem and conjecture its solution in the region of parameter space bounded from below by the curve $I$ and from above by $M$, defined by (4.6). We shall denote this region by $\mathcal{TMR}$. In Figure 18 we show the corresponding uniform shock configurations, related sonic curves and the important variables.

As in von Neumann reflection, the solution in this case has the constant

value $U_2$ left of the shock $S_2$ up to the sonic parabola $P_2$. Then $S_2$ becomes nonuniform; we again call it $\widetilde{S_2}$. We assume that, as in von Neumann reflection, the shock strength of $\widetilde{S_2}$ is decaying, that is, the subsonic solution $u$, left of the shock $\widetilde{S_2}$, is decreasing as we move away from $P_2$. We shall assume that at the point, $\widetilde{\Xi_I}$, where $\widetilde{S_2}$ meets $S_1$, the state on the left of $\widetilde{S_2}$ is sonic. This is the only scenario that leads to the existence of a solution for the parameter values belonging to the region $\mathcal{TMR}$. However, unlike the case of von Neumann reflection, the shock strength at $\widetilde{\Xi_I}$ is not zero. Rather, at the point $\widetilde{\Xi_I}$ where the shock waves $S_1$ and $\widetilde{S_2}$ intersect, a degenerate hyperbolic wave interaction occurs. This degenerate hyperbolic interaction is the same as the one occurring for parameter values on the curve $I$ (see the Remark at the end of Section 3). The following general result shows that the configuration of shock polars corresponds to region 4, and therefore there is a unique admissible solution which consists of a $-$-rarefaction wave, a constant state, $U_m$, and a $+$-shock wave between $U_m$ and $U_0$.

**Proposition 4.4** *Let $a \geq 1/\sqrt{2}$ and suppose that $\widetilde{\Xi_I}$ is any point on $S_1$. Then there is a unique value $U_D$ on $S^+(U_1, \widetilde{\Xi_I})$ which is sonic at $\widetilde{\Xi_I}$. (The first condition means that $U_D$ belongs to the $+$-shock branch of the downstream locus of $U_1$ at $\widetilde{\Xi_I}$.) Furthermore, there is a unique solution of the quasi-one-dimensional Riemann problem at $\widetilde{\Xi_I}$ with data $U_0$ and $U_D$, consisting of a shock beween $U_0$ and an intermediate state $U_m$, and a rarefaction wave between $U_m$ and $U_D$.*

**Proof:** Since $\widetilde{\Xi_I}$ is on $S_1$, we have

$$\widetilde{\xi_I} = a\widetilde{\eta_I} + \frac{1}{2} + a^2$$

and if $U_D$ is sonic then

$$u_D = \frac{\widetilde{\eta_I}^2}{4} + \widetilde{\xi_I}.$$

We can use these two equations to write

$$\frac{\widetilde{\eta_I}}{2} = -a + \sqrt{u_D - \frac{1}{2}}. \tag{4.7}$$

We note that if $a \geq 1/\sqrt{2}$, then there is a one-to-one correspondence between values $u_D \geq 1/2 + a^2 \geq 1$ and points on $S_1$ with $\widetilde{\eta_I} \geq 0$. Now $U_D \in S^+(U_1, \widetilde{\Xi_I})$ implies

$$v_D + a = (u_D - 1)\left(\frac{\widetilde{\eta_I}}{2} - \sqrt{\frac{\widetilde{\eta_I}^2}{4} + \widetilde{\xi_I} - \frac{u_D + u_1}{2}}\right) \tag{4.8}$$

(from the shock polar equation, (3.5), with $U_1 = (1, -a)$). Using (4.7) here, we obtain an equation for $v_D$ in terms of $u_D$:

$$v_D = u_D \frac{\widetilde{\eta_I}}{2} - \sqrt{u_D - \frac{1}{2}} - \frac{(u_D - 1)^{3/2}}{\sqrt{2}} .$$

Now, in order for the Riemann problem between $U_0$ and $U_D$ to have a unique solution consisting of a $+$-shock and a $-$-rarefaction wave, $U_D$ must lie in region 4 of the downstream locus of $U_0$. To verify that $U_D$ is in region 4, we compute the $v$-coordinates of the two sonic points on the shock loop $S(U_0, \widetilde{\Xi_I})$ and show that they bracket $v_D$. Using (3.5) again with $U_0 = (0, 0)$, we get

$$v_{max,min} = u_D \left( \frac{\widetilde{\eta_I}}{2} \pm \sqrt{\frac{\widetilde{\eta_I}^2}{4} + \widetilde{\xi_I} - \frac{u_D}{2}} \right) = u_D \left( \frac{\widetilde{\eta_I}}{2} \pm \sqrt{\frac{u_D}{2}} \right) .$$

We require $v_{min} \leq v_D \leq v_{max}$; taking into account the expressions for $v_{max}$, $v_{min}$ and $v_D$, we see the second inequality is always satisfied, and the first is equivalent to $F(u_D) \leq 0$ where

$$F(u) \equiv \sqrt{u - \frac{1}{2}} + \frac{(u-1)^{3/2}}{\sqrt{2}} - \frac{u^{3/2}}{\sqrt{2}}.$$

Calculating the derivative of $F$ one sees that $F'(u) < 0$ on $[1, \infty)$. Therefore, since $F(1) = 0$, $F$ is negative for all $u_D > 1$. This completes the proof. ■

We summarize our candidate for a transitional Mach reflection in the following conjecture, illustrated in Figure 19.

**Conjecture** If $(a, b) \in \mathcal{TMR}$ there will be a solution that consists of an incident shock, a reflected wave that meets the incident shock at a point $\widetilde{\Xi_I}$ above the wall, a Mach stem and a rarefaction wave emanating from $\widetilde{\Xi_I}$. The incident shock is uniform up to $\widetilde{\Xi_I}$, the reflected wave is uniform up to $\Xi_0$, transonic and nonuniform from $\Xi_0$ to $\widetilde{\Xi_I}$, and sonic at $\widetilde{\Xi_I}$. The rarefaction wave and Mach stem have the same structure as in the degenerate Case 1 problem arising along the curve $I$ in $(a, b)$-parameter space.

Therefore, there is a small hyperbolic region consisting of a state $U_m$ and a rarefaction wave between $U_D$ and $U_m$ that penetrates the region of subsonic flow. This is also seen in numerical experiments in [10].

### 4.4 A MECHANISM FOR MACH REFLECTION WITH A KINK

In this section we conjecture the structure of the solution in the the region of $(a, b)$-parameter space that lies above the curve $M$, right of the line

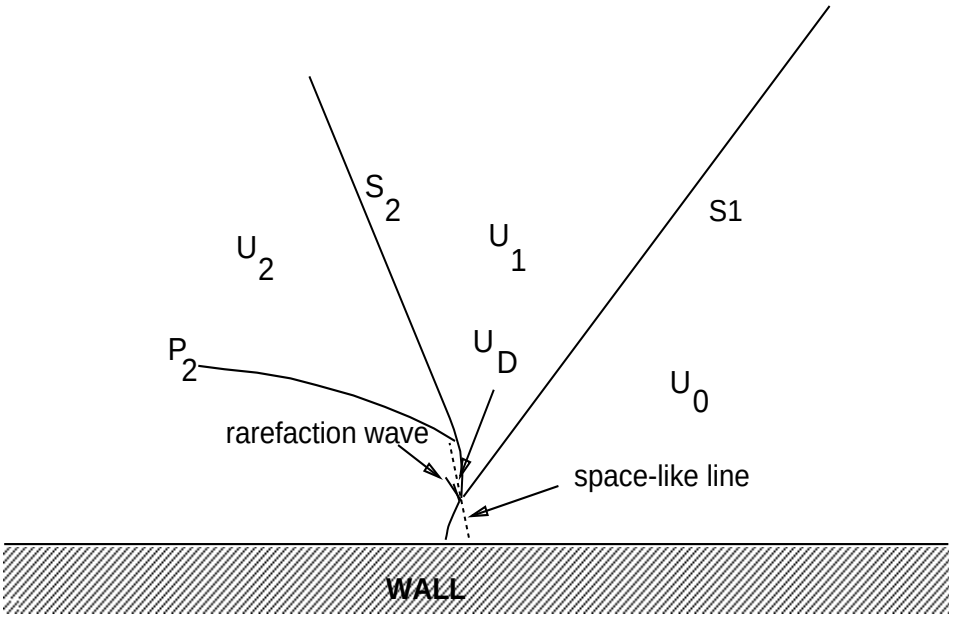


**Figure 19:** Transitional Mach Reflection

$a = 1/\sqrt{2}$, and left of the line $a = \sqrt{2}$. We call this region $\mathcal{KMR}$ because the structure of the solution we will describe in this section is a prototype of *kinky Mach reflection*.

The solution here is similar to the solution in region $\mathcal{TMR}$. Our solution consists of the constant state $U_2$ on the left of $S_2$ until $S_2$ reaches $\Xi_0$, the point of intersection with the parabola $P_2$. Then $S_2$ becomes nonuniform; call it again $\widetilde{S_2}$. The position of this transonic shock is determined by solving a free-boundary problem (the Rankine-Hugoniot conditions determine the position of the free boundary). The intersection of $S_1$ and $\widetilde{S_2}$ occurs at a point above the wall (since we are left of $a = \sqrt{2}$ in parameter space), with $\widetilde{S_2}$ having nonzero strength (because $a > 1/\sqrt{2}$). Again, let $\widetilde{\Xi_I} = (\widetilde{\xi_I}, \widetilde{\eta_I})$ denote the point of intersection between $\widetilde{S_2}$ and $S_1$, with $\widetilde{\eta_I} > 0$. We conjecture the following scenario for this interaction.

The shock $\widetilde{S_2}$, having traversed a subsonic region, is sonic again at the point, $\widetilde{\Xi_I}$, where it meets $S_1$, and is such that the resulting degenerate hyperbolic quasi-one-dimensional Riemann problem can be solved in the positive time-like direction. If this is the case, locally we have a degenerate hyperbolic quasi-one-dimensional Riemann problem of the same type as in the case of transitional Mach reflection. Again, by Proposition 4.4, at the point $\widetilde{\Xi_I}$ on $S_1$ there is a unique point $U_D$ on the shock locus $S(U_1, \widetilde{\Xi_I})$ which is downstream from $U_1$ and is sonic at $\widetilde{\Xi_I}$. The degenerate Riemann

problem at $\widetilde{\Xi_I}$ with data $U_D$ and $U_0$ will again have a solution consisting of a shock and a rarefaction wave. The difference between this configuration and the prototype for transitional Mach reflection is that when $b >> 1$, the requirement that $\widetilde{S_2}$ approaches $\widetilde{\Xi_I}$ in the positive time-like direction in the neighborhood of $\widetilde{\Xi_I}$ implies that the shock $\widetilde{S_2}$ changes curvature from being concave up just beyond the point $\Xi_0$ where $S_2$ meets $P_2$ to being concave down near $\widetilde{\Xi_I}$, This is why we call this solution a kinky Mach reflection. If $(a, b)$ is near the curve $M$, this configuration resembles transitional Mach reflection.

## 5. Conclusions

We now have a scenario for the wave interaction for every point in the $(a, b)$-parameter space, summarized in Figure 20. In the bifurcation diagram there are three curves that serve as sharp boundaries between different types of wave interactions. These are the curve $I$ that serves as the boundary of Case 1, the region in the parameter space for which hyperbolic wave interactions take place (see Theorem 3.2); the line $a = \sqrt{2}$, on the left of which no symmetric shock reflection at the wall is possible (see Proposition 4.2); and the curve $a = J(b)$ along which uniform regular reflection takes place (see Proposition 4.3). Other regions may overlap and for those parameters the change between different types of wave interactions is smooth.

If we compare the proposed wave interactions, by region, with the theoretical and experimental predictions of Ben-Dor, [1] (see especially Figures 2.39, 2.41b, 2.45b and several of the later figures), we see there is a rough correspondence between the 'bifurcation diagram' in the $(M_s, \theta_{\rm w}^C)$ plane and the one that we are building in the $(a, b)$ plane: the $(M_s, \theta_{\rm w}^C)$ diagram must be rotated 90 degrees counterclockwise and then reflected in a vertical axis for the correspondence to be apparent. The diagrams differ in some details like the persistence of the simple Mach reflection (SMR) region for large $M_s$ (not necessarily supported by experiment) and the failure of SMR to occur at small $M_s$ for large and small $\theta_{\rm w}^C$. However, as a qualitative picture of what this model may be capable of showing, namely the relation between different types of two-dimensional wave interactions as parameters vary, our picture shows some success: von Neumann reflection and regular reflection are far apart; in fact, they span the parameter space, and are separated by all the other modes of interaction. A significant difference is that there is a region devoted to 'double Mach reflection' in Ben-Dor's experimental and theoretical descriptions. Double Mach reflection may not occur in our simple model. We note, however, that the model was designed to describe transition between regular, von Neumann and simple Mach reflection at low

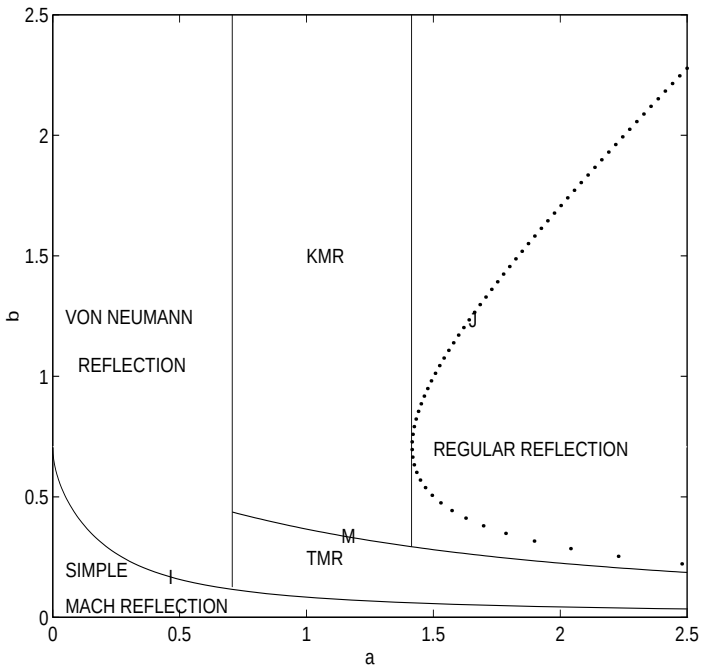


**Figure 20:** Wave Interaction Bifurcation Diagram

Mach numbers, where double Mach reflection does not occur, in theory. In our model, the strip $1/\sqrt{2} \leq a \leq \sqrt{2}$ contains transitional and kinky Mach reflection for large values of $b$ and we conjecture that there is no further transition to double Mach reflection.

Our simplified model does not contain 'triple points' (see [3]). Of course, the full gas dynamics equations do not contain triple points either: a so-called triple point really consists of four states and four discontinuities, one being a slip line. However, our model does not permit slip lines. Here it may be noteworthy that no experimental results show a triple point with uniform states in all four quadrants: the flow behind the triple point is always nonuniform (though, on the scale of the problem, it may be close to constant). The simple Mach reflection which we described in Section 3.3 (Theorem 3) is the nearest this model comes to a triple point. Our candidate for Mach reflection is in fact a hyperbolic quasi-one-dimensional Riemann problem: there are four states rather than three and there is a small rarefaction wave as well as three shocks. This is exactly what the numerical simulations in [10] for Case 1 data indicate. (The calculations reported by Brio and Hunter, [3], do not include any Case 1 points.)

We have not yet completed the task of proving existence of the conjectured solutions to the free-boundary problems we have posed here. How-

ever, we have some evidence, from the solutions we have found to their fixed-boundary counterparts, that solutions do exist. The progress we have made in classifying different types of interaction patterns and the transitions between them supports our theme that shock interaction phenomena cannot be understood without examination of the full solution of the equations, particularly in the subsonic region. We believe that the paradoxes and their resolutions which appear in this simplified model have their counterparts, *mutatis mutandis*, in the full equations of gas dynamics.

## References

[1] G. Ben-Dor. *Shock Wave Reflection Phenomena*. Springer-Verlag, New York, 1992.

[2] B. Boston. Front tracking of complex wave interactions. *Ph.D. Thesis*, SUNYSB-AMS-95-12, 1995.

[3] M. Brio and J. K. Hunter. Mach reflection for the two dimensional Burgers equation. *Physica D*, 60:194–207, 1992.

[4] S. Čanić and B. L. Keyfitz. A free-boundary problem for the two-dimensional unsteady transonic small disturbance equation. In preparation.

[5] S. Čanić and B. L. Keyfitz. Quasi-one-dimensional Riemann problems and their role in self-similar two-dimensional problems. UH Mathematics Department Research Report UH-MD-218, 1996, submitted to SIAM Journal of Mathematical Analysis.

[6] S. Čanić and B. L. Keyfitz. An elliptic problem arising from the unsteady transonic small disturbance equation. *Journal of Differential Equations*, 125:548–574, 1996.

[7] S. Čanić and B. L. Keyfitz. A smooth solution for a Keldysh type equation. *Communications in Partial Differential Equations*, 21:319–340, 1996.

[8] S. Čanić and B. L. Keyfitz. Oblique shock interactions and the von Neumann paradox. In *Proceedings of the 20th International Conference on Shock Waves, Caltech (1995)*, In press.

[9] S. Čanić, B. L. Keyfitz, and D. H. Wagner. A bifurcation diagram for oblique shock interactions in the unsteady transonic small disturbance

equation. In J. Glimm et al., editors, *Proceedings of the Fifth International Conference on Hyperbolic Problems: Theory, Numerics, and Applications*, pages 178–187. World Scientific, Singapore, 1996.

[10] S. Čanić and D. Mirković. A numerical study of shock reflection modeled by the unsteady transonic small disturbance equation. Submitted to SIAM Journal of Applied Mathematics.

[11] P. Colella and L. Henderson. The von Neumann paradox for the diffraction of weak shock waves. *Journal of Fluid Mechanics*, 213:71–94, 1990.

[12] H. M. Glaz. Self-similar shock reflection in two space dimensions. In J. Glimm and A. Majda, editors, *Multidimensional Hyperbolic Problems and Computations*, volume IMA, 29, pages 89–106. Springer, New York, 1991.

[13] H. M. Glaz, P. Colella, I. I. Glass, and R. L. Deschambault. A numerical study of oblique shock-wave reflections with experimental comparisons. *Proceedings of the Royal Society of London*, A398:117–140, 1985.

[14] L. F. Henderson. Regions and boundaries for diffracting shock wave systems. *Zeitschrift für Angewandte Mathematik und Mechanik*, 67:73–86, 1987.

[15] A. Sakurai, L. Henderson, K. Takayama, Z. Walenta, and P. Colella. On the von Neumann paradox of weak Mach reflection. *Fluid Dynamics Research*, 4:333–346, 1989.

[16] R. J. Virgona. A study of shock wave diffraction from regular to irregular reflection and the effects of gas viscoisty. *Ph. D. Thesis, University of Sydney*, 1993.